Prediction of the Quasistatic Planar Motion of a Contacted Rigid Body

J.C. Trinkle
Department of CS
Texas A&M University
College Station, TX 77843-3112
trink@cs.tamu.edu

D.C. Zeng
Department of CS
Georgia Institute of Technology
Atlanta, GA 30332
czeng@cc.gatech.edu

November 1, 1994

Abstract

Planning the motion of bodies in contact requires a model of contact mechanics in order to predict sliding, rolling, and jamming. Such a model typically assumes that the bodies are rigid and that tangential forces at the contacts obey Coulomb's law. Though, usually assumed to be constant, the static and dynamic coefficients of friction vary in space and time and are difficult to measure accurately. In this paper, we study a quasistatic, multi-rigid-body model for planar systems, in which the coefficients of friction are treated as independent variables. Our analysis yields inequalities defining regions in the space of friction coefficients for which a particular contact mode (*i.e.*, a particular combination of sliding, rolling, or separating at the contacts) is feasible. The geometrical interpretation of these inequalities leads to a simple graphical technique to test contact mode feasibility. This technique is then used to generate a nontrivial example in which several contact modes are simultaneously feasible. Despite model ambiguity, there are factors which argue in favor of using a quasistatic, rigid-body model. This point is highlighted by the successful application of our results to the planning of two manipulation tasks.

1 Introduction

Planning whole-arm manipulation, assembly, and other contact tasks to be carried out by robotic systems involves predicting the motions of systems of bodies with multiple points of contact. The positions and orientations of some of the bodies (the links of the manipulator) are actively controlled while the other bodies (the workpieces) move only in response to the motions of the actively controlled bodies. The goal of planning is to determine a sequence of manipulator motion and force commands which, if executed, would achieve a prespecified relative arrangement of all the bodies (*e.g.*, a new grasp or completed assembly). In general, achieving this desired arrangement requires the commanded actions to take advantage of sliding, rolling, and separating at existing contacts, and the establishment of new contacts. Therefore the model employed by such a planner must allow for the possibility of sliding and rolling at every contact in the system. We study such a model here.

Given the goal of developing a planner for the class of systems outlined above, one is faced with a difficult modeling decision. If the bodies are assumed rigid and the friction forces obey Coulomb's Law, then the motion of the system cannot always be uniquely predicted (see for example see [2, 13, 24]). If, on the other hand, the bodies are assumed to be compliant, then the motion of the system and the contact forces can always be uniquely predicted [11, 43]. This feature is desirable when it comes to simulation and planning. However, predictions rely on estimates of the effective compliance and friction coefficients at each contact. The compliance coefficients can be determined through finite element analyses, but due to the computational demand, one would not want a planner to have to perform finite element analyses for each (significantly different) system configuration considered during planning. In addition, if the compliance values do not reflect those of the real system, motion prediction could be erroneous and lead to plans which fail for no apparent reason. Therefore, we advocate modeling the bodies as rigid. While it is true that the assumption of rigidity is simply an assumption of zero contact compliance, we prefer this assumption to other choices, because it has been used to produce plans which agree with the observed gross behavior of multibody systems and less computation is required to predict the system motion (see [3, 5, 8, 9, 10, 16, 17, 18, 21, 28, 29, 40, 44] for examples).

Given that a multi-rigid-body model is to be used, the question remaining is whether or not to model dynamic effects. This choice is task dependent. If the task is to be done as quickly as possible, dynamic effects must be included. If not, a quasistatic model, one which ignores inertial forces, may prove a viable alternative. An advantage of choosing a quasistatic model is that planning is less time consuming. This is true, because the dynamic model depends on velocities appearing in the Coriolis and centripedal acceleration terms. Therefore the dynamic model is sensitive to the magnitudes of the velocity variables. In an approximate cell-decomposition approach the space of velocity variables must be discretized. While this discretization does not necessarily have to be fine [34], some discretization that captures the system's sensitivity to velocity must be used.

A second discretization of the velocity space is implied by the dependence of the contact

forces on relative velocities at the contacts. For each possible set of maintained contacts (this set is not known *a priori*), one must divide the velocity space into regions corresponding to all possible combinations of leftward or rightward sliding or rolling at each contact. This discretization, when superimposed on the first, yields even more cells than either discretization alone. The advantage of using a quasistatic model is that the first discretization is unnecessary. Then, having generated a path based on a quasistatic model, an appropriate execution speed for the path can be determined by using a dynamic model and dynamic time-scaling techniques similar to those applied in [30] and [34].

In this paper, a quasistatic, planar, multi-rigid-body model allowing sliding and rolling at multiple frictional contacts is explored. Since the coefficients of friction in real systems are sensitive to load and difficult to control factors, such as dirt and moisture in the contact interfaces [23], the quasistatic model is studied with particular attention paid to gross variations in its solutions as a function of the coefficients of friction at the contacts. The friction model can be viewed as Coulomb's Law with friction coefficients varying in space and time.

The contributions of this paper are: (1) a set of mathematical conditions under which our model is most useful, (2) a procedure for partitioning the joints of the manipulator into position- and torque-controlled subsets, and (3) the derivation of analytical relationships defining regions in the space of friction coefficients in which the model predicts a particular contact mode or set of contact modes, where a contact mode is the association of a specific interaction (sliding, rolling, or separating) with each contact point. These contributions in concert with our examples of manipulation using sliding and rolling contacts lead to a better understanding of quasistatic multi-rigid-body models.

2 Background

This paper focuses on the formulation and solution of a general quasistatic model of rigid, planar, whole-arm manipulation systems, so that it may be used effectively in future research on planning tasks involving contact. Therefore, the ensuing discussion is organized in a way which, first, emphasizes different aspects of quasistatic and dynamic multi-rigid-body models, and second, relates previous work in manipulation planning to the corresponding aspects of these models.

2.1 Quasistatic vs. Dynamic Contact Problems

The dynamic multi-body contact problem is to determine the motion of a system of bodies in contact given the state of the system (the positions and velocities of all the bodies) at the time of interest. The goal is to determine the accelerations of the bodies and the force at each contact. Usually one formulates the equations of motion of the bodies, the nonpenetration constraints (initially written in terms of the positions of the bodies), and a friction law at

the contacts. This results in a system of differential algebraic equations and inequalities in the contact forces and the accelerations of the bodies (for example, see [2, 13, 37]). Next one differentiates the nonpenetration constraints twice with respect to time to write them in terms of the system's unknown accelerations. Finally, the resulting system of equations and inequalities is solved for the accelerations and the contact forces, taking into account the complementary nature of contact forces and relative contact accelerations and velocities (*i.e.*, when a contact separates, the contact force must be zero, *etc.*).

Notice that in the dynamic problem, the nonpenetration constraints are differentiated twice; just enough times to write them in terms of the highest order time derivative appearing in the Newton-Euler equations. Quasistatic contact problems have been solved analogously, but the quasistatic assumption leads to a fundamental difference. Since inertial forces are neglected, the Newton-Euler equations no longer contain the accelerations of the bodies. This means that the highest order derivatives of the body positions are the velocities that appear in the Coulomb friction constraints. Therefore, the relevant kinematic constraints are obtained by differentiating the nonpenetration constraints only once. A further consequence is that the only couplings between the unknown force and motion variables are through Coulomb's Law.

The abovementioned fundamental difference between the quasistatic and dynamic multi-rigid-body models manifests itself in the problem formulations and applicable solution techniques. For example, the three-dimensional, frictionless, quasistatic problem may be formulated as a linear program [41], while the analogous dynamic problem cannot. It can be formulated as a positive definite linear complementarity problem or equivalent positive definite quadratic program [2]. In the frictional case with sliding and rolling contacts, both problems become significantly more difficult to solve. The dynamic problem becomes a nonlinear complementarity problem [25], while the quasistatic problem takes the form of an uncoupled nonlinear complementarity problem (achieving this form requires a straight forward extension of the formulation given in [26]).

2.2 Model Indeterminacy and Inconsistency

The dynamic and quasistatic models discussed above both suffer from indeterminacy in motion prediction, *i.e.,* they can admit several contact modes for a given state and input even when all physical and geometric parameters are known precisely. Parameter uncertainty exaggerates this problem. The models can also be inconsistent even when the kinematic constraints by themselves are not. For example, a rigid rod in one-point contact with a rigid table can have zero, one, two, or three finite force solutions under the dynamic model [13] and no solution at all in the quasistatic case. An example of a quasistatic problem with multiple solutions is discussed in Subsection 4.3.

The predominant approach to dealing with model inconsistencies has been to ignore them, since they appear to be quite rare [2, 31]. Indeterminacies are more common and have

been dealt with in manipulation planning by delimiting all such situations and then avoiding them [7]. An alternative is to plan in a way that ensures that the desired goal is reached despite uncertainty in the exact system motion, which Brost accomplished in two ways [3]. He used energy arguments to plan placing-by-dropping tasks and state transition cones to plan pushing tasks.

The first planning approach, avoiding indeterminate situations, has motivated several researchers (most notably Erdmann [7], Rajan *et al.* [31], and Brost and Mason [4]) to attempt to categorize all situations in which multi-body models are indeterminate. Erdmann found that the three-dimensional motion of a body in contact with its environment is indeterminate if the C-space friction cone for a one-contact situation dips below the tangent plane at the contact point on the C-obstacle in C-space. Also, Erdmann stated (on page 251 of [7]) *...when the edges of the individual friction cones which comprise a composite friction cone are not coplanar, then a variety of reaction forces can arise in response to an applied force. Effectively, the distribution of reaction forces among the points of contact is indeterminate. Consequently, the resulting motion is ambiguous.* However, we warn the reader that nonuniqueness in the contact force distribution does not necessarily imply nonuniqueness in the system motion. For example, the acceleration of frictionless systems are unique even when the contact force distribution is not [14]).

Rajan, Burridge, and Schwartz studied and classified the indeterminate dynamic planar motion of a single rigid body in contact with two fixed rigid "walls" [31] (Note that in this paper, the "walls" can move and there can be any number of them). The result was a simplicial decomposition of the three-dimensional space of external wrenches (a wrench is a force and moment taken together), with each simplex corresponding to a possible contact mode. Under certain circumstances, the simplices overlapped, indicating that more than one contact mode was consistent with the system model. Note however, that the work by Rajan *et al.* and Erdmann does not carry over directly to the quasistatic case. This fact was highlighted by Rajan *et al.* who refer to a "forthcoming" paper containing the analogous results for the quasistatic case, but unfortunately that paper was never published. The work presented here helps to fill the gap left by Rajan *et al.*

In contrast to the analyses of Erdmann and Rajan *et al.*, Brost and Mason developed a graphical technique referred to as "moment labeling" [4, 20]. This technique allows one to easily determine the feasibility of a specific contact mode for a planar body in contact with any number of points fixed in the environment. In planning situations, moment labeling is carried out for every possible contact mode to determine the set of lines of action of the external force for which only the desired contact mode satisfies the model. Then the desired contact mode can be executed by applying a force from within this set.

The relationship between Brost's and Mason's results and ours becomes evident after specializing moment-labeling to the quasistatic case. The result of applying the moment-labeling technique is a directed channel through which the line of action of the end effector force must pass in order to be consistent with the desired contact mode. Brost's and Mason's technique identifies the regions outside the channel, whereas our technique identifies the

inside of the channel. Despite the equivalence of our analytical approach and their graphical approach, it would be impractical to derive the moment-labeling approach from our analytical results. However, graphical moment-labeling is limited to planar systems, while our analytical approach can be extended in a straight forward manner to three-dimensional systems with multiple workpieces.

2.3 The Utility of Quasistatic Models

Mason [19] and Peshkin [27] proposed that the "scope" of quasistatic models be delimited by the ratio of the moment of inertia of a pushed object to the square of the pushing velocity. However, since their results are not readily extensible to spatial systems or general planar systems, we take a different view, which we refer to as quasistatic model *utility*.

We view the failure of the quasistatic model in the case of the rigid rod in one-point contact with a table, as a result of the equilibrium equation's requirement that the external wrench applied to the rod (*i.e.*, force and moment) be a member of a lower-dimensional subset of the space of all wrenches. In the rigid rod problem, the quasistatic model can only have a solution if the line of action of the gravitational force passes through the contact point. Since it does not, the rod moves dynamically. This observation suggests that quasistatic analysis will be most "useful" if, in each configuration, the contact forces can balance all likely external wrenches, so that the system never accelerates. Due to uncertainty in the system's physical and geometric parameters, the set of likely wrenches will have the same dimension as the space of all wrenches.

Now, consider a multi-rigid-body system with multiple contacts that can balance every wrench in a full-dimensional set of likely external wrenches. Each wrench corresponds to a different contact force distribution (or set of distributions when the contact forces are statically indeterminate). The conjecture, which motivates our definition of model utility, is that as the applied wrench is varied within the set, the contact force distribution changes to maintain equilibrium.

This sort of quasistatic behavior has been observed and exploited in several previous studies. In one study by Trinkle and Hunter [39], a polygon was to be reoriented within a simple planar hand. In every configuration comprising the plan, the contact forces could balance a three-dimensional set of likely external wrenches, thereby making the plan robust to uncertainty in the position of the center of mass of the workpiece. No significant dynamic behavior was observed in experiments [40]. The same characteristics were present in earlier work done by Trinkle on how to lift a part off of a table top without causing excessive contact forces between the part and the table top [42].

Lynch's work on stable quasistatic pushing [16], provides a second example. The problem he studied was to push a part (called a "slider") on a horizontal plane in such a way as to maintain sticking contact with the pusher at two points. In this problem, the specific wrench to generate a specific slider motion was indeterminate, because the force distribution

between the horizontal support plane and the part was unknown. However, the slider was to maintain contact with the pusher at two distinct sticking points. This was possible, because as the slider moved, the varying friction wrench was equilibrated by corresponding variations of the contact forces between the pusher and slider (within their friction cones). Therefore, the motion of the pusher uniquely defined the motion of the slider (this behavior was experimentally verified).

Previous work in "quasistatic" manipulation planning that violates our utility conditions possess one of the following characteristics: (1) the quasistatic analysis is used initially to determine an equilibrium configuration after which dynamic analysis is used to determine the system motion; (2) there are too few contact constraints to maintain equilibrium once achieved, but the system is dynamically stable; or (3) there are two few contact constraints to maintain equilibrium, but the system is unstable.

An example of quasistatic analysis followed by dynamic analysis is Simunovic's work on planar peg insertion with two sliding contacts. He found that for insertion to proceed quasistatically, the external force (applied by the manipulator to the peg) had to pass through the point of intersection of the contact forces applied by the hole [38]. Since control errors and uncertainty make the application of such a force impossible, Simunovic up-graded his model to a dynamic one to determine his main result; a recipe for choosing the direction and line of action of the applied force to guarantee acceleration into the hole. Note that the quasistatic assumption required the external wrench to lie in a two-dimensional subset of the wrench space, while the conditions found with the dynamic model allowed the external wrench to be chosen from a three-dimensional subset. Nonetheless, the quasistatic result was important, because it defined the boundary between applied wrenches that would cause acceleration into the hole and those that would cause jamming.

An example of a dynamically stable system gainfully analyzed through a quasistatic model is Peshkin's fence layout planning for conveyor-belt parts-orienting systems [28]. In this sort of system, a part will typically develop two sliding or one rolling contact with a fence. Thus it is only possible to balance a two-dimensional subset of the three-dimensional space of wrenches that could be applied to the part by the conveyor belt. However, in the real system, parts were observed translating at a constant speeds with two contacts sliding along the fence. The motion was quasistatic, because perturbations in the velocity of the part along the fence were resisted by the belt and perturbations away from the fence were removed since the belt had a component of velocity toward the fence. Other similar useful quasistatic analyses of dynamically stable systems include the squeeze-grasping work of Brost [3] and Goldberg [10], the fixture insertion of Schimmels and Peshkin [36], and Whitney's reformulation of previous peg-in-hole work leading to the design of the RCC device [44].

Examples of unstable system productively analyzed through a quasistatic model are Mason's and Peshkin's early work on planar pushing with one contact [18, 27]. We classify such pushing actions as unstable, because as the slider is pushed, it does not maintain its relative position with respect to the pusher. Nonetheless, such problems can benefit from quasistatic analysis, because friction effects dominate inertial forces. The experimental

results of Mason and Peshkin clearly show that the quasistatic analysis is still useful in these situations, but the information content of the results is diluted. For example, in Lynch's stable pushing work, discussed above, the pusher trajectory completely determined the slider trajectory, whereas with one point pushing, the slider trajectory could only be bounded.

2.4 Paper Layout

In Section 3, our quasistatic model is presented along with an approach to solving it based on contact modes (*i.e.*, various combinations of sliding, rolling, and separating at the contacts). We also introduce conditions for model utility and a technique to decide the control modes of the joints of the manipulator. In Section 4, regions of the space of friction coefficients (μ-space) for which different contact modes are feasible are defined as inequalities of rational functions in the coefficients of friction and a graphical interpretation of the inequalities is presented. We then discuss a nontrivial configuration for which three distinct contact modes are simultaneously feasible. In Section 5, two examples of our quasistatic analysis are studied. In the first example, we show how our analysis can be applied to a system with nonconstant coefficients of friction. The second example contains configurations for which the quasistatic model is ambiguous. However, for that specific example, we show how the ambiguity can be resolved by the proper control of internal forces. Finally, in Section 6, conclusions and suggestions for future research are given.

3 Problem Formulation

A rigid laminar body of arbitrary shape (the *workpiece*) moves quasistatically in a plane due to frictional contact with one or more actively-controlled, rigid, laminar bodies. The actively controlled bodies can be viewed as the links of a *manipulator* composed of any number of serial and branching kinematic chains. The joints are either revolute or prismatic. The manipulator and the workpiece are collectively referred to as the *system*. We assume that:

1. The positions, orientations, and geometries of all bodies are known.
2. The bodies are rigid and restricted to move in a plane.
3. The external wrenches applied to all the bodies in the system (other than those due to contacts) are known.
4. The kinetic energy of the system and all dynamic effects are negligible.
5. Each joint may be position- or effort-controlled; effort control implies force control of a prismatic joint and torque control of a revolute joint.

6. The friction forces at the contacts are Coulombic in nature with unknown, possibly different, coefficients.

Then, given the instantaneous velocities of a subset of joints and the efforts applied at the remaining joints, our goal is to determine the instantaneous velocity of the workpiece satisfying the quasistatic model. We would also like to determine the contact forces and the unspecified joint efforts and velocities. Finally, we want to show how the solution depends on the coefficients of friction at the contact points.

To formulate the governing equations, a "world" frame may be chosen arbitrarily. For convenience, we choose it so that its origin coincides with the center of gravity of the workpiece (see Figure 1). One contact frame is assigned to each contact point and is positioned

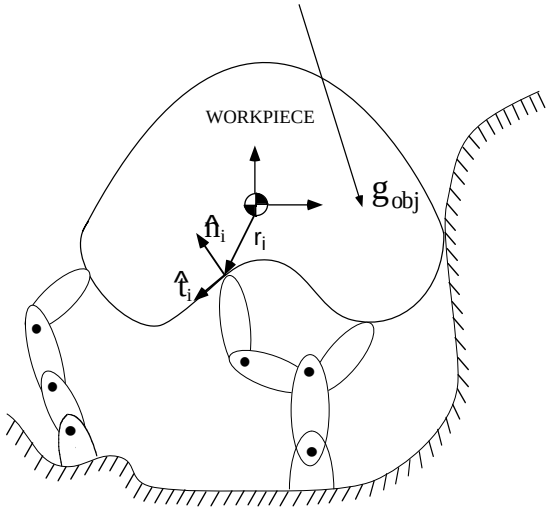

Figure 1: Workpiece in Contact with Manipulator

with its origin at the contact point and with its "n"-axis, $\hat{\mathbf{n}}_i$, aligned with the contact normal (pointing inward with respect to the workpiece), its "t"-axis, $\hat{\mathbf{t}}_i$, aligned with the contact tangent such that the cross product of $\hat{\mathbf{n}}_i$ and $\hat{\mathbf{t}}_i$, points out of the plane of motion.

Let the vector $\mathbf{c}_i = [c_{in} \quad c_{it}]^T$ represent the force applied to the workpiece at the i^{th} contact such that c_{in} and c_{it} are the normal and tangential components, where ^{T} indicates matrix transposition. The vector $\mathbf{c}_i$ is known as the wrench intensity vector [35] of the i^{th} contact. The wrench matrix, $\mathbf{W}_i$, transforms the i^{th} contact force into the world frame. In the planar case, $\mathbf{W}_i$ is defined as follows:

$$\mathbf{W}_i = [\mathbf{w}_{in} \quad \mathbf{w}_{it}] = \begin{bmatrix} \hat{\mathbf{n}}_i & \hat{\mathbf{t}}_i \\ \mathbf{r}_i \otimes \hat{\mathbf{n}}_i & \mathbf{r}_i \otimes \hat{\mathbf{t}}_i \end{bmatrix}_{(3\times 2)} ; \ \forall i \in \{1, \ldots, n_c\} \tag{1}$$

where $\hat{\mathbf{n}}_i$, $\hat{\mathbf{t}}_i$, $\mathbf{r}_i$ are all expressed in the world coordinate frame, $\mathbf{r}_i$ is the position of the i^{th} contact point, the $\otimes$ operator applied to two vectors, $[a_1, a_2] \otimes [b_1, b_2]$, is defined as $a_1 b_2 - a_2 b_1$,

the subscript $_{(3\times 2)}$ indicates the dimension of the matrix, and n_c is the number of distinct contact points.

Let $\mathbf{g}_{obj}$ be the external wrench applied to the workpiece; it includes all forces and moments not applied at the contact points whose normals lie in the plane of motion. Thus $\mathbf{g}_{obj}$ can include wrenches resulting from gravity and sliding contact with a supporting plane. Summing all the wrenches yields the equations of equilibrium:

$$\mathbf{W}\mathbf{c} + \mathbf{g}_{obj} = \mathbf{W}_n\mathbf{c}_n + \mathbf{W}_t\mathbf{c}_t + \mathbf{g}_{obj} = \mathbf{0} \tag{2}$$

where $\mathbf{W}$ and $\mathbf{c}$ are known as the global wrench matrix and the global wrench intensity vector [12] and have dimensions $(3 \times 2n_c)$ and $(2n_c \times 1)$, respectively. The normal and tangential wrench matrices, $\mathbf{W}_n$ and $\mathbf{W}_t$, both of dimension $(3 \times n_c)$, are formed by the horizontal concatenation of all the individual normal and tangential contact wrenches $\mathbf{w}_{in}$ and $\mathbf{w}_{it}$ (defined in equation (1)). Correspondingly, the normal and tangential wrench intensity vectors, $\mathbf{c}_n$ and $\mathbf{c}_t$, both have length n_c and are formed by the vertical concatenation of all the normal and tangential wrench intensity components, c_{in} and c_{it}, respectively.

The manipulator must satisfy its equilibrium equations [12]:

$$\mathbf{J}^T\mathbf{c} = \mathbf{J}_n^T\mathbf{c}_n + \mathbf{J}_t^T\mathbf{c}_t = \boldsymbol{\tau} - \mathbf{g}_{man} \tag{3}$$

where $\mathbf{J}$ is the concatenation of the individual manipulator Jacobians for the points of contact, expressed in their respective contact frames, $\boldsymbol{\tau}$ is the vector of joint efforts, and $\mathbf{g}_{man}$ is the vector of joint efforts induced by external wrenches acting on the manipulator links. The partitions $\mathbf{J}_n$ and $\mathbf{J}_t$ are exactly analogous to the partitions $\mathbf{W}_n$ and $\mathbf{W}_t$, of the wrench matrix, $\mathbf{W}$.

The motion of the workpiece is subject to kinematic velocity constraints, the satisfaction of which implies that the point bodies do not penetrate the workpiece's boundary. Denoting the relative linear velocity at the i^{th} contact expressed with respect to the i^{th} contact frame as $\mathbf{v}_i = [v_{in} \;\; v_{it}]^T$, then the nonpenetration constraint is given by the following inequality:

$$v_{in} \geq 0; \quad \forall i \in \{1, \ldots, n_c\}. \tag{4}$$

Note that the quasistatic nonpenetration constraint is a function only of system velocities for the reason given in Subsection 2.1.

Let $\dot{\mathbf{q}} = [\dot{q}_x \quad \dot{q}_y \quad \dot{q}_\theta]^T$ represent the linear and angular velocity of the point on the workpiece coincident with the origin of the world frame, then $\mathbf{W}_i^T\dot{\mathbf{q}}$ is the linear velocity of the i^{th} contact point on the workpiece expressed with respect to the i^{th} contact frame [12]. The linear velocity of the i^{th} contact point on the manipulator may be written as the product of the Jacobian matrix (excluding the rows corresponding to rotational velocity) associated with the point, $\mathbf{J}_i = \left[\begin{array}{c} \mathbf{j}_{in} \\ \mathbf{j}_{it} \end{array} \right]_{(2\times n_\theta)}$, [6] and the joint velocity vector, $\dot{\theta}$, of length n_θ,

the number of joints of the manipulator. Thus the relative linear velocity at the i^{th} contact expressed in the i^{th} contact frame is given by:

$$\mathbf{W}_i^T \dot{\mathbf{q}} - \mathbf{J}_i \dot{\theta} = \mathbf{v}_i \; ; \quad \forall i \in \{1, \ldots, n_c\}. \tag{5}$$

Writing constraints (4) in matrix form yields:

$$\mathbf{W}_n^T \dot{\mathbf{q}} - \mathbf{J}_n \dot{\theta} \geq \mathbf{0} \tag{6}$$

where $\mathbf{J}_n$ was formed by vertically concatenating the rows, $\mathbf{j}_{in}$, of the individual contact Jacobian matrices, $\mathbf{J}_i$.

The remaining constraints enforce the Coulomb friction model, which for the planar case, may be written as a system of linear inequalities as follows:

$$\mathbf{Bc} \geq \mathbf{0} \tag{7}$$

where

$$\mathbf{B} = \begin{bmatrix} \mathbf{U} & \mathbf{I} \\ \mathbf{U} & -\mathbf{I} \end{bmatrix}_{(2n_c \times 2n_c)} , \qquad \mathbf{c} = \begin{bmatrix} \mathbf{c}_n \\ \mathbf{c}_t \end{bmatrix}_{(2n_c \times 1)} , \tag{8}$$

$\mathbf{U} = diag\{\mu_1, \ldots, \mu_{n_c}\}$ is the diagonal matrix of effective coefficients of friction, and $\mathbf{I}$ is the $(n_c \times n_c)$ identity matrix. Note that inequality (7) implicitly constrains the contact forces to be nontensile (*i.e.*, $c_{in} \geq 0; \;\; \forall\, i$).

To complete our model, we introduce complementary constraints relating the contact force components with the relative contact velocity components for the three possible types of contact interactions:

Rolling contact:

$$v_{in} = v_{it} = 0, \;\; c_{in} \geq 0, \;\; -\mu_i c_{in} \leq c_{it} \leq \mu_i c_{in}; \;\; \forall i \in \mathcal{R} \tag{9}$$

Sliding contact:

$$v_{in} = 0, \; c_{in} \geq 0, \;\; \left\{ \begin{array}{ll} v_{it} < 0, & c_{it} = \mu_i c_{in} \\ v_{it} > 0, & c_{it} = -\mu_i c_{in} \end{array} \right\}; \;\; \forall i \in \mathcal{S} \tag{10}$$

Breaking contact:

$$v_{in} > 0, \;\; c_{in} = 0, \; c_{it} = 0; \;\; \forall i \in \mathcal{B} \tag{11}$$

where the disjoint sets, $\mathcal{R}$, $\mathcal{S}$, and $\mathcal{B}$, contain the indices of the contacts assumed to be rolling, sliding, and breaking, respectively.

We now can state the quasistatic motion prediction problem more precisely. Given: (1) the values of a subset of the elements in the joint velocity vector, $\dot{\theta}$, (2) the values of the complementary elements in the joint effort vector $\boldsymbol{\tau}$, and (3) the relevant geometric and physical information encoded in $\mathbf{W}$, $\mathbf{J}$, $\mathbf{B}$, $\mathbf{g}_{obj}$, and $\mathbf{g}_{man}$. Determine: (1) the velocity of the workpiece, $\dot{\mathbf{q}}$, (2) the unspecified elements of the vectors $\boldsymbol{\tau}$ and $\dot{\theta}$, (3) and, if possible, the vector of contact force components, $\mathbf{c}$.

3.1 A Solution Approach

To find the solution(s) to our quasistatic model, we must check the feasibility of every possible contact mode. Since each contact may slide, roll, or separate, there are at most 3^{n_c} (where n_c is the number of contact points) contact modes. When n_c is large, most of these contact modes violate the corresponding kinematic constraints, so many modes may be rejected before computing contact forces and joint efforts. Also, when the manipulator's joints are not moving, the right hand term on the left side of inequality (4) becomes zero. Then the number of contact modes can be shown to be of order n_c^2 [20].

Let the selection matrices, $\mathbf{E}_R$, $\mathbf{E}_S$, and $\mathbf{E}_B$, identify the currently considered contact mode. Each matrix consists of a stack of row vectors, $\mathbf{e}_i^T$, of length n_c, with the i^{th} element equal to 1 and all others 0:

$$\mathbf{E}_R = \begin{bmatrix} \vdots \\ \mathbf{e}_i^T \\ \vdots \end{bmatrix}_{(n_R \times n_c)} ; \ \forall i \in \mathcal{R} \qquad \mathbf{E}_S = \begin{bmatrix} \vdots \\ \mathbf{e}_i^T \\ \vdots \end{bmatrix}_{(n_S \times n_c)} ; \ \forall i \in \mathcal{S} \qquad \mathbf{E}_B = \begin{bmatrix} \vdots \\ \mathbf{e}_i^T \\ \vdots \end{bmatrix}_{(n_B \times n_c)} ; \ \forall i \in \mathcal{B} \tag{12}$$

where n_R, n_S, and n_B are the numbers of contacts assumed to be rolling, sliding, and breaking, respectively. Note that we have not explicitly separated the cases of leftward and rightward sliding as some previous authors have. This is because our conditions for model utility (derived below) imply that the directions of sliding are uniquely determined.

Given an hypothesized contact mode, the corresponding set of "applicable" kinematic constraints can be written as follows:

$$\mathbf{W}_A^T \dot{\mathbf{q}} - \mathbf{J}_A \dot{\theta} = \mathbf{0}. \tag{13}$$

The applicable wrench and Jacobian matrices, $\mathbf{W}_A^T$ and $\mathbf{J}_A$ are:

$$\mathbf{W}_A^T = \begin{bmatrix} \mathbf{W}_{nR}^T \\ \mathbf{W}_{tR}^T \\ \mathbf{W}_{nS}^T \end{bmatrix}_{((2n_R+n_S)\times 3)}, \qquad \mathbf{J}_A = \begin{bmatrix} \mathbf{J}_{nR} \\ \mathbf{J}_{tR} \\ \mathbf{J}_{nS} \end{bmatrix}_{((2n_R+n_S)\times n_\theta)}, \tag{14}$$

where $\mathbf{W}_{nR}^T = \mathbf{E}_R \mathbf{W}_n^T$, and $\mathbf{J}_{nR} = \mathbf{E}_R \mathbf{J}_n$, with $\mathbf{W}_{tR}$, $\mathbf{W}_{nS}$, $\mathbf{J}_{tR}$, and $\mathbf{J}_{nS}$ defined similarly. The matrices $\mathbf{W}_{tR}^T$ and $\mathbf{J}_{tR}$ appearing in the the matrices $\mathbf{W}_A^T$ and $\mathbf{J}_A$ constrain the relative linear velocity at the rolling contacts to be zero.

The contacts assumed to be breaking must satisfy the following inequality:

$$\mathbf{W}_{nB}^T \dot{\mathbf{q}} - \mathbf{J}_{nB} \dot{\theta} > \mathbf{0} \tag{15}$$

where $\mathbf{W}_{nB}^T = \mathbf{E}_B \mathbf{W}_n^T$ and $\mathbf{J}_{nB} = \mathbf{E}_B \mathbf{J}_n$.

The wrench intensity vectors of the sliding contacts are known to lie along the edges of their respective friction cones. To write these constraints in matrix form, we define the diagonal tangential directions matrix, $\mathbf{\Xi}$, as follows:

$$\mathbf{\Xi} = diag\{\xi_1, \ldots, \xi_{n_c}\} \tag{16}$$

where $\xi_i = sgn(\mathbf{w}_{it}^T\dot{\mathbf{q}} - \mathbf{j}_{it}\dot{\theta})$, $sgn()$ is the signum function, and $\mathbf{w}_{it}$ and $\mathbf{j}_{it}$ were defined in the previous section. Given these definitions, the sliding tangential wrench intensity vector has length n_S and is given by:

$$\mathbf{c}_{tS} = -\mathbf{U}_S\mathbf{\Xi}_S\mathbf{c}_{nS} \tag{17}$$

where $\mathbf{c}_{nS} = \mathbf{E}_S\mathbf{c}_n$, $\mathbf{U}_S = \mathbf{E}_S\mathbf{U}\mathbf{E}_S^T$, $\mathbf{\Xi}_S = \mathbf{E}_S\mathbf{\Xi}\mathbf{E}_S^T$, and $\mathbf{c}_{tS} = \mathbf{E}_S\mathbf{c}_t$.

Substituting equation (17) into the equilibrium equation (2) yields:

$$\mathbf{W}_{A\mu}\mathbf{c}_A = (\mathbf{W}_A + \mathbf{W}_{\mu S})\mathbf{c}_A = -\mathbf{g}_{obj} \tag{18}$$

where $\mathbf{W}_{\mu S}$ and the applicable wrench intensity vector, $\mathbf{c}_A$, are given as:

$$\mathbf{W}_{\mu S} = [\mathbf{0} \quad -\mathbf{W}_{tS}\mathbf{U}_S\mathbf{\Xi}_S] \qquad \mathbf{c}_A = \begin{bmatrix} \mathbf{c}_{nR} \\ \mathbf{c}_{tR} \\ \mathbf{c}_{nS} \end{bmatrix}_{((2n_R+n_S)\times 1)}. \tag{19}$$

Here $\mathbf{W}_{tS} = \mathbf{W}_t\mathbf{E}_S^T$ has dimension $(3 \times n_S)$ and $\mathbf{0}$ has dimension $(3 \times 2n_R)$.

Rewriting the manipulator equilibrium equations and Coulomb constraints in terms of the applicable wrench intensity vector yields:

$$\mathbf{J}_{A\mu}^T\mathbf{c}_A = (\mathbf{J}_A^T + \mathbf{J}_{\mu S}^T)\mathbf{c}_A = \boldsymbol{\tau} - \mathbf{g}_{man} \tag{20}$$

$$\mathbf{B}_A\mathbf{c}_A \geq \mathbf{0} \tag{21}$$

where $\mathbf{J}_{\mu S}^T$ and $\mathbf{B}_A$ are defined as:

$$\mathbf{J}_{\mu S}^T = [\mathbf{0} \quad -\mathbf{J}_{tS}^T\mathbf{U}_S\mathbf{\Xi}_S] \qquad \mathbf{B}_A = \begin{bmatrix} \mathbf{U}_R & \mathbf{I}_R & \mathbf{0} \\ \mathbf{U}_R & -\mathbf{I}_R & \mathbf{0} \\ \mathbf{0} & \mathbf{0} & \mathbf{I}_S \end{bmatrix}_{((2n_R+n_S)\times(2n_R+n_S))}. \tag{22}$$

Here, the dimensions of the submatrices $\mathbf{0}$ and $\mathbf{J}_{tS}^T\mathbf{U}_S\mathbf{\Xi}_S$ of $\mathbf{J}_{\mu S}^T$ are $(n_{jnts} \times 2n_R)$ and $(n_{jnts} \times n_S)$, respectively, the matrices $\mathbf{I}_R$ and $\mathbf{I}_S$ are the n_R- and n_S-dimensional identity matrices, respectively, and $\mathbf{J}_{tS}^T = \mathbf{J}_t^T\mathbf{E}_S^T$, and $\mathbf{U}_R = \mathbf{E}_R\mathbf{U}\mathbf{E}_R^T$. Note that inequality (22) constrains the elements of $\mathbf{c}_{nR}$ to be nonnegative through the friction cone constraints in the upper (2×2) block partition of $\mathbf{B}_A$. However, the submatrix $\mathbf{I}_S$ is needed to prevent elements of $\mathbf{c}_{nS}$ from becoming negative, because equation (17) does not guarantee nonnegativity.

3.2 Model Utility and Joint Control Mode Partitioning

The utility of the model formulated above, lies in its ability to accurately predict the quasistatic motion of the system. At the very least, we demand for each possible contact mode, that the quasistatic model predict the velocity of the workpiece uniquely. As discussed in Subsection 2.3, this requires that the contact forces be able to balance all external wrenches

in a three-dimensional set of possible external wrenches. However, we would prefer the somewhat more stringent utility condition that for a given contact mode, the model be able to predict all of the the contact forces and joint efforts uniquely. In this section, we derive conditions necessary to meet these utility conditions. However, we recognize that the second condition, namely, that the contact forces and joint efforts can be uniquely determined, is overly restrictive in some situations (*e.g.,* Lynch's stable pushing work [15]). Therefore, at the end of this subsection, we will indicate how to relax this condition.

Consider first the velocity kinematic relationships corresponding to a given contact mode (equation (13)). The velocity, $\dot{\mathbf{q}}$, of the workpiece can be determined uniquely if we can identify a $((2n_R+n_S)\times(2n_R+n_S))$ nonsingular partition, $\mathbf{P}_{A_I}$, of the matrix $[\mathbf{W}_A^T \quad -\mathbf{J}_A]$:

$$\mathbf{P}_{A_I} = [\mathbf{W}_A^T \quad -\mathbf{J}_A\mathbf{E}_{P_{A_I}}^T]_{((2n_R+n_S)\times(2n_R+n_S))} \tag{23}$$

where $\mathbf{E}_{P_{A_I}}^T$ is a matrix that selects (if possible) the appropriate column(s) of $\mathbf{J}_A$. The solution of the applicable kinematic constraints is then:

$$\dot{\mathbf{z}}_I = -\mathbf{P}_{A_I}^{-1}\mathbf{P}_{A_{II}}\dot{\mathbf{z}}_{II} \tag{24}$$

where $\mathbf{P}_{A_{II}} = -\mathbf{J}_A\mathbf{E}_{P_{A_{II}}}^T$, $\mathbf{E}_{P_{A_{II}}}^T$ selects all columns of $\mathbf{J}_A$ not selected by $\mathbf{E}_{P_{A_I}}^T$, $\dot{\mathbf{z}}_I = [\dot{\mathbf{q}}^T \quad \dot{\theta}^T\mathbf{E}_{P_{A_I}}^T]^T$, and $\dot{\mathbf{z}}_{II} = \mathbf{E}_{P_{A_{II}}}\dot{\theta}$.

Equation (24) provides a partitioning of the vector of joint velocities into input and output portions based on the requirement that for a given input, $\dot{\mathbf{q}}$ must be unique. Here $\dot{\mathbf{z}}_{II}$ is the parition of $\dot{\theta}$ viewed as input and $\dot{\mathbf{z}}_I$ is the output containing $\dot{\mathbf{q}}$ and the remaining elements of $\dot{\theta}$. Equation (24) also implies two mathematical conditions necessary for model utility: first, the number of kinematic equality constraints, $2n_R+n_S$, must be between 3 and $3+n_\theta$, inclusive, and second, the rank of $\mathbf{W}_A^T$ must be three.

In order for the solution implied by equation (24) to be kinematically admissible, the contacts presumed to break (by the choice of the contact mode) must separate. Rewriting inequality (15) leads to the following constraint on the input vector, $\dot{\mathbf{z}}_{II}$:

$$(\mathbf{P}_{nB_{II}} - \mathbf{P}_{nB_I}\mathbf{P}_{A_I}^{-1}\mathbf{P}_{A_{II}})\dot{\mathbf{z}}_{II} > \mathbf{0}. \tag{25}$$

where $\mathbf{P}_{nB_I} = [\mathbf{W}_{nB}^T \quad -\mathbf{J}_{nB}\mathbf{E}_{P_{A_I}}^T]$ and $\mathbf{P}_{nB_{II}} = -\mathbf{J}_{nB}\mathbf{E}_{P_{A_{II}}}^T$.

Our second condition for model utility is that we be able to uniquely determine all of the unspecified joint efforts and applicable wrench intensities. However, taking all elements of $\mathbf{c}_A$ and $\boldsymbol{\tau}$ as unknown, the equilibrium equations, (2) and (3), are potentially underdetermined. Partitioning them to identify a nonsingular $((2n_R+n_S)\times(2n_R+n_S))$ submatrix $\mathbf{Q}_{A_I}$ of $\mathbf{Q}_{A_I} = [\mathbf{W}_{A\mu}^T \quad \mathbf{J}_{A\mu}]^T$ yields the following equations:

$$\mathbf{c}_A = \mathbf{Q}_{A_I}^{-1}\begin{bmatrix} -\mathbf{g}_{obj} \\ -\mathbf{g}_{man_I} + \boldsymbol{\tau}_I \end{bmatrix} \tag{26}$$

$$\boldsymbol{\tau}_{II} = \mathbf{Q}_{A_{II}}\mathbf{Q}_{A_I}^{-1}\begin{bmatrix} -\mathbf{g}_{obj} \\ -\mathbf{g}_{man_I} + \boldsymbol{\tau}_I \end{bmatrix} + \mathbf{g}_{man_{II}} \tag{27}$$

where $\mathbf{Q}_{A_I} = [\mathbf{W}_{A\mu}^T \quad \mathbf{J}_{A\mu}\mathbf{E}_{Q_{A_I}}^T]^T$, $\mathbf{Q}_{A_{II}} = \mathbf{E}_{Q_{A_{II}}}\mathbf{J}_{A\mu}^T$, $\mathbf{g}_{man_I} = \mathbf{E}_{Q_{A_I}}\mathbf{g}_{man}$, $\mathbf{g}_{man_{II}} = \mathbf{E}_{Q_{A_{II}}}\mathbf{g}_{man}$, $\boldsymbol{\tau}_I = \mathbf{E}_{Q_{A_I}}\boldsymbol{\tau}$, and $\boldsymbol{\tau}_{II} = \mathbf{E}_{Q_{A_{II}}}\boldsymbol{\tau}$. The vectors $\mathbf{c}_A$ and $\boldsymbol{\tau}_{II}$ are uniquely determined by equations (26) and (27) when $\boldsymbol{\tau}_I$ is given. Therefore, we view $\boldsymbol{\tau}_I$ as input.

As was the case in the preceeding kinematic analysis, the equilibrium analysis implies two conditions necessary for model utility. The first one is identical to one implied by the kinematic analysis, namely, $2n_R + n_S$ must be between 3 and $3 + n_\theta$, inclusive. The second condition, which is implied by the nonsingularity of $\mathbf{Q}_{A_I}$, is that the rank of $\mathbf{W}_{A\mu}$ must be three.

In order for the solution implied by equations (26) and (27) to be consistent with the assumed contact interactions associated with the given contact mode, the constraints implied by the Coulomb friction model given in inequality (21) must be satisfied. Substituting equation (26) into inequality (21) yields:

$$\mathbf{B}_A\mathbf{Q}_{A_I}^{-1}\begin{bmatrix} \mathbf{0} \\ \boldsymbol{\tau}_I \end{bmatrix} \geq \mathbf{B}_A\mathbf{Q}_{A_I}^{-1}\begin{bmatrix} \mathbf{g}_{obj} \\ \mathbf{g}_{man_I} \end{bmatrix}. \tag{28}$$

In summary, the above kinematic and equilibrium analyses have identified a partition $\dot{\mathbf{z}}_{II}$ of the joint velocity vector and a partition $\boldsymbol{\tau}_I$ of the joint effort vector as input. In other words, we have identified a control mode partitioning for the manipulator; the joints corresponding to elements of $\boldsymbol{\tau}_I$ and $\dot{\mathbf{z}}_{II}$ are to be effort-controlled and velocity-controlled[1], respectively. However, for this control mode partitioning to be valid, the sets of joints corresponding to $\boldsymbol{\tau}_I$ and $\dot{\mathbf{z}}_{II}$ must be disjoint and their union must be the set of all joints. Therefore $\mathbf{E}_{P_{A_I}}$ and $\mathbf{E}_{Q_{A_I}}$ must be identical.

The conditions for quasistatic model utility are:

$$3 \leq 2n_R + n_S \leq 3 + n_\theta \tag{29}$$

$$Rank(\mathbf{W}_A) = 3 \tag{30}$$

$$Rank(\mathbf{W}_{A\mu}) = 3 \tag{31}$$

$$\exists\ \mathbf{E}_{P_{A_I}} = \mathbf{E}_{Q_{A_I}} \ni \mathbf{P}_{A_I}^{-1}\ and\ \mathbf{Q}_{A_I}^{-1}\ exist. \tag{32}$$

Clearly, these conditions restrict the number of sets of maintained contacts to be considered during the solution process to less than 3^{n_c} (see Table 1).

As mentioned at the beginning of this subsection, the condition that the contact forces and joint efforts be determinate can be overly restrictive. For example, the contact forces are statically indeterminate when there are two rolling contacts between the workpiece and a link of the manipulator. More generally, the contact forces are statically indeterminate

[1]Velocity control can be accomplished either directly with a velocity-based servo-system or by shaping the reference input to a position controller.

when $\mathbf{Q}_A$ has a nontrivial null space. In such cases, the above derivation generally follows the same line, but requires the use of generalized matrix inversion. Relaxing this condition would impact the mathematical expressions of the utility conditions (29-32). The right-hand inequality in inequality (29) would no longer apply and both references to $\mathbf{Q}_{A_I}$ would be dropped from equation (32) in favor of the constraint that left null space of $\mathbf{Q}_{A_I}$ have dimension zero.

In keeping with previous robotics literature, we henceforth refer to control mode partitions with at least one effort-controlled joint as compliant control modes and those with no effort-controlled joints as noncompliant control modes. Therefore, noncompliant control mode partitions arise when the number of kinematic constraints associated with the hypothesized contact mode is equal to three (*i.e.*, when $2n_R + n_S = 3$).

4 Decomposition of μ-Space

In this section, we analyze all quasistatic contact modes satisfying our utility conditions, equations (29-32). In doing so, we have found it convenient to partition the possible contact modes according to the numbers and types of contact interactions. Recall that contact modes for which $2n_R + n_S$ is equal to three, are noncompliant modes. These are easiest to analyze, because the number of kinematic constraint equations is smallest. Also, because no joints require effort-control, a manipulator capable of noncompliant control is simpler to implement. For these reasons, we concentrate on the noncompliant contact modes. These modes must have either three sliding contacts with all other contacts breaking or one sliding and one rolling contact, all others breaking; we denote these contact modes by $3S$ and RS. The compliant contact modes, $2R$, $R2S$, $4S$, $2RS$, $R3S$, $5S$, *etc.*, are discussed only briefly.

For a given contact mode, the kinematic and equilibrium requirements for quasistatic motion are completely specified by equations (24-28). In the following subsections, it is assumed that the kinematic constraints (24 and 25) are met, so we can focus on the details of the μ-space constraints.

4.1 Regions in μ-Space for $3S$ Modes

The quasistatic contact modes denoted by $3S$ are most likely to occur when the coefficients of friction are small. The mode-defining matrices and vectors are:

$$\mathbf{Q}_{A_I} = \mathbf{W}_{A\mu} = (\mathbf{W}_{nS} - \mathbf{W}_{tS}\mathbf{\Xi}_S\mathbf{U}_S) \qquad \mathbf{c}_A = \mathbf{c}_{nS} \qquad \mathbf{B}_A = \mathbf{I}. \tag{33}$$

Substituting into inequality (28) yields the following system of inequalities in the coefficients of friction:

$$c_{nSi} = \frac{E_i \prod_{j \neq i} \mu_j + \sum_{j \neq i} F_{i,j}\mu_j + G_i}{A\mu_1\mu_2\mu_3 + B_1\mu_2\mu_3 + B_2\mu_1\mu_3 + B_3\mu_1\mu_2 + C_1\mu_1 + C_2\mu_2 + C_3\mu_3 + D} \geq 0;$$

$$\forall i \in \{1,2,3\} \tag{34}$$

where the coefficients, A, B_i, C_i, D, E_i, F_{ij}, and G_i, can be written as determinants of three-by-three matrices multiplied by up to three nonzero elements of the tangential directions matrix (see Appendix A for definitions). Thus the analytical expressions for the regions of a valid $3S$ motion in μ-space are as follows:

$$\left\{ \begin{array}{l} A\mu_1\mu_2\mu_3 + B_1\mu_2\mu_3 + B_2\mu_1\mu_3 + B_3\mu_1\mu_2 + C_1\mu_1 + C_2\mu_2 + C_3\mu_3 + D > 0 \\ E_i \prod\limits_{j\neq i} \mu_j + \sum\limits_{j\neq i} F_{i,j}\mu_j + G_i \geq 0 \; ; \qquad \forall i \in \{1,2,3\} \end{array} \right\} \tag{35}$$

or

$$\left\{ \begin{array}{l} A\mu_1\mu_2\mu_3 + B_1\mu_2\mu_3 + B_2\mu_1\mu_3 + B_3\mu_1\mu_2 + C_1\mu_1 + C_2\mu_2 + C_3\mu_3 + D < 0 \\ E_i \prod\limits_{j\neq i} \mu_j + \sum\limits_{j\neq i} F_{i,j}\mu_j + G_i \leq 0 \; ; \qquad \forall i \in \{1,2,3\} \end{array} \right\} \tag{36}$$

It is important to note that the coefficients of the inequalities, and therefore the $3S$ regions in μ-space, are dependent on $\dot{\theta}$ through the elements of the tangential directions matrix, $\mathbf{\Xi}$ (see equation (16)). Thus, $3S$ motion of the workpiece in one direction, $\dot{\theta}$, may be possible for "large" coefficients of friction, while $3S$ motion in the opposite direction, $-\dot{\theta}$, may only be possible for "small" friction coefficients.

Figure 2 below shows an arbitrary arrangement of three contacts on a laminar workpiece. Its shape is arbitrary as long as its boundary contains the origins of the three contact frames and is tangent to the $\hat{\mathbf{t}}$ axes at those points. The external wrench shown acts through the center of mass as the gravitational and effective friction forces would if the workpiece were sliding on an inclined plane; it is assumed to be given by, $\mathbf{g}_{obj} = [0 \quad -1 \quad 0]^T$. The linear velocities of the contact points on the manipulator expressed in the contact frames are assumed to be $\mathbf{J}_1\dot{\theta} = [0.920 \quad -0.391]^T$, $\mathbf{J}_2\dot{\theta} = [0.928 \quad -0.375]^T$, and $\mathbf{J}_3\dot{\theta} = [-0.931 \quad -0.367]^T$. These velocities are shown as arrows labeled, $\mathbf{J}_i\dot{\theta}$; $\forall i \in \{1,2,3\}$. The wrench matrix is given by:

$$\mathbf{W} = [\mathbf{w}_{1n} \;\; \mathbf{w}_{1t} \;\; \mathbf{w}_{2n} \;\; \mathbf{w}_{2t} \;\; \mathbf{w}_{3n} \;\; \mathbf{w}_{3t}] = \begin{bmatrix} 0.804 & -0.595 & -0.707 & -0.707 & -0.973 & 0.232 \\ 0.595 & 0.804 & 0.707 & -0.707 & -0.232 & -0.973 \\ 1.04 & -20.9 & -3.50 & -17.9 & 14.0 & -7.63 \end{bmatrix} \tag{37}$$

Figure 3 shows four slices of the contact mode regions in μ-space taken perpendicular to the μ_3-axis. The areas in the μ_1-μ_2 planes containing the 1's represent slices of the $3S$ region. The areas containing the 2's belong to the RS region (to be analyzed in the next subsection) corresponding to contact "1" rolling, contact "2" sliding, and contact "3" breaking. Note that the $3S$ region shrinks as the coefficient of friction at the third contact increases, but the RS region is uneffected, because the only the first and second contacts are involved with that contact mode.

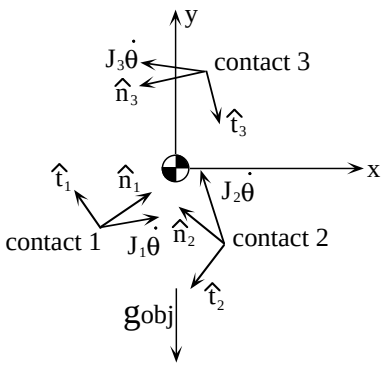

Figure 2: Configuration with Feasible $3S$ Mode

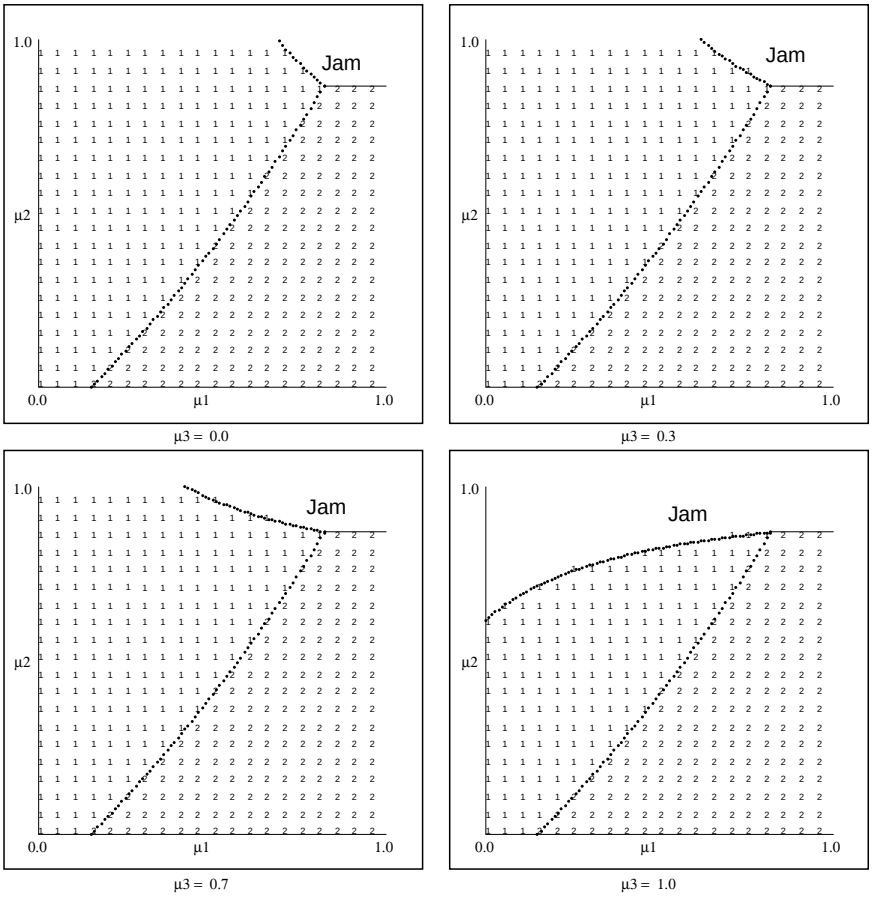

Figure 3: μ-Space Decomposition for Configuration shown in Previous Figure

The dotted curve with positive slope belongs to both the $3S$ and RS regions. Thus the RS and $3S$ regions are not disjoint; the solution to our quasistatic model is not unique. However, if we were to modify inequality (9), so that during rolling, the contact force had to lie strictly within the friction cone, then the dotted curve would be a part of the $3S$ region and not the RS region. While this simple fix would resolve the nonuniqueness problem encountered in this example, in the Subsection 4.3, we discuss an example for which such a simple fix would not resolve ambiguities.

The areas labeled "Jam" in Figure 3 indicate that no contact mode (with nonzero system velocity) is feasible. In this particular case, for every contact mode with feasible kinematic constraints, contact friction prevents the motion. In addition, equilibrium is possible when the input velocities, $\mathbf{J}_i\dot{\theta}$, are set to zero.

Inequalities (35) and (36) embody the feasibility of the equilibrium and Coulomb constraints given the presumed contact mode. As pointed out by Zeng [45], they also have a simple graphical interpretation which we paraphrase as follows:

Corollary 1 *Assume that there are n_c contacts, $n_c \geq 3$. Consider a set of three contacts and assume that the kinematic velocity constraints implied by the sliding of those three contacts are satisfied. Further assume that the matrix, $\mathbf{W}_{A\mu}$, is nonsingular. Then it is feasible that all the three contacts in question slide simultaneously if and only if the following two conditions are satisfied:*

- *The direction of the external force must be an element of the negative span of the three contact forces in question.*
- *For each set of two contacts, the lines of actions of the external wrench and the other contact wrench must produce moments of opposite sense about the intersection point of the lines of action of the paired contacts.*

These conditions are analogous to the form closure[2] conditions derived by Nguyen [22] for static planar grasps. However, because the three contacts are sliding, there are only have three constraining unisense wrenches. Therefore, form closure is impossible. Instead, the contacts are maintained by the action of the external wrench; the situation referred to as "force closure" by Reuleaux [33] and Salisbury [35].

Figure 4 illustrates the graphical interpretation of the conditions stated in the Corollary and embodied in inequalities (35) and (36). It requires knowledge of the lines of action and the directions of the contact forces, which are known assuming that the joint velocity vector, $\dot{\theta}$, the coefficients of friction[3], and the contact geometry are known.

The assumption that $\mathbf{W}_{A\mu}$ is nonsingular implies that the lines of action of the three contact wrenches do not intersect at a point. Therefore, they form the triangle, $\triangle p_{12}p_{23}p_{31}$.

[2]Nguyen called this condition "force closure."

[3]We assume here, for illustrative purposes only, that the coefficients of friction are known.

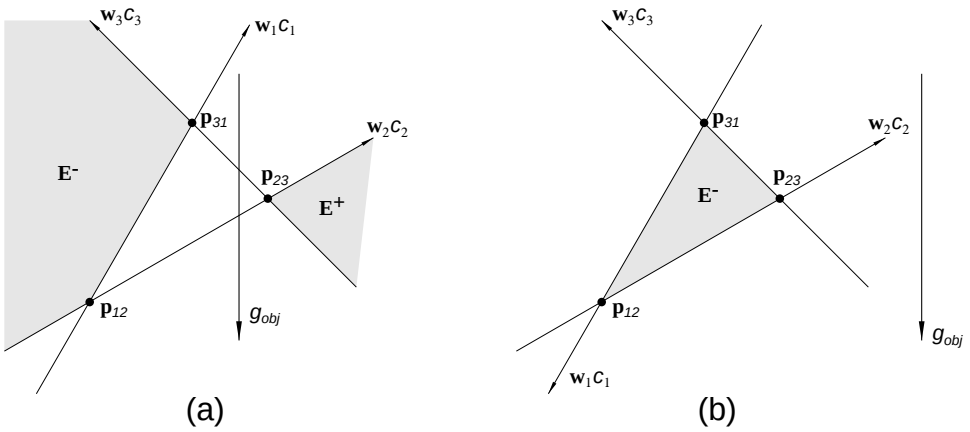

Figure 4: Illustrations of Necessary and Sufficient Conditions for the Existence of a $3S$ Solution.

There are two qualitatively distinct cases illustrated in Figures 4(a) and 4(b). In (a), the contact forces do not positively span the plane; in (b) they do.

In the case in which the contact forces do not positively span the plane (see Figure 4(a)), there always exists a pair of contact wrenches whose lines of action intersect at a vertex of $\triangle p_{12}p_{23}p_{31}$ such that they point toward the other vertices. Label these contact wrenches, $\mathbf{w}_1 c_1$ and $\mathbf{w}_2 c_2$ and vertex, p_{12}. The other contact wrench is $\mathbf{w}_3 c_3$. For 3S mode feasibility, the Corollary requires the line of action of the external wrench (labeled $\mathbf{g}_{obj}$) to pass through the interiors of the segments $\overline{p_{23}p_{31}}$ and $\overline{p_{12}p_{23}}$ with the line of action directed from $\overline{p_{23}p_{31}}$ to $\overline{p_{12}p_{23}}$ as shown in Figure 4(a). Notice that the positive cone formed by the wrench pair $\mathbf{w}_1 c_1$ and $\mathbf{w}_2 c_2$ and the pair $\mathbf{w}_3 c_3$ and $\mathbf{g}_{obj}$ "see each other," satisfying Nguyen's form closure condition. Also, in this figure, we have shaded the $\mathbf{E}^+$ and $\mathbf{E}^-$ regions produced by applying Brost's and Mason's moment-labeling technique. For the quasistatic contact mode to be feasible, the external wrench, $\mathbf{g}_{obj}$ must generate a positive moment with respect to $\mathbf{E}^+$ and a negative moment with respect to $\mathbf{E}^-$. In other words, the line of action of $\mathbf{g}_{obj}$ must pass through the unshaded channel. Note that our condition for mode feasibility is equivalent to Brost's and Mason's condition found through moment-labeling.

In the case for which the contact forces positively span the plane (see Figure 4(b)), no pair of the lines of action, intersect such that both point toward other vertices of the triangle. In this case, the Corollary requires that the line of action of the external wrench create a moment with respect to every point in the triangle in the sense opposite to that produced by the three contact wrenches. Nguyen's technique still applies. Having met our condition, any pairing of the four wrenches yields two cones whose positive (or negative) spans contain the apex of the other cone. With regard to the moment-labeling technique, this case results in only one labeled region; either $\mathbf{E}^+$ or $\mathbf{E}^-$ and that the region is the interior of triangle $\triangle p_{12}p_{23}p_{31}$. Note again that our conditions are equivalent to Brost's and Mason's.

4.2 Regions in μ-Space for RS

The other type of noncomplaint contact mode is the RS mode. For RS modes, we have the following definitions:

$$\mathbf{Q}_{A1} = \mathbf{W}_{A\mu} = [\mathbf{w}_{nR} \quad \mathbf{w}_{tR} \quad (\mathbf{w}_{nS} - \xi_S \mu_S \mathbf{w}_{tS})] \qquad \mathbf{c}_{A1} = \begin{bmatrix} c_{nR} \\ c_{tR} \\ c_{nS} \end{bmatrix} \qquad \mathbf{B}_A = \begin{bmatrix} \mu_R & 1 & 0 \\ \mu_R & -1 & 0 \\ 0 & 0 & 1 \end{bmatrix} \tag{38}$$

where μ_R and μ_S are the coefficients of friction at the rolling and sliding contacts and ξ_S is the direction of relative tangential velocity at the sliding contact (see equation (16) for definition). Again, as in the $3S$ case, $\mathbf{Q}_{A2}$ and $\mathbf{c}_{A2}$ are degenerate.

Substituting the definitions (38) into equation (26) yields:

$$c_{nR} = \frac{C_1\mu_S + D_1}{A\mu_S + B}, \qquad c_{tR} = \frac{C_2\mu_S + D_2}{A\mu_S + B}, \qquad c_{nS} = \frac{D_3}{A\mu_S + B} \tag{39}$$

where the coefficients A, B, C_i, and D_i, can be written as three-by-three determinants multiplied by up to three nonzero elements of the tangential directions matrix (see Appendix B for definitions). Substituting the wrench intensities into the Coulomb friction constraint (21) yields the analytical expressions for the region of μ-space in which the chosen RS contact mode exists:

$$\left\{ \begin{array}{l} A\mu_S + B > 0 \\ C_1\mu_R\mu_S + D_1\mu_R - C_2\mu_S - D_2 \geq 0 \\ C_1\mu_R\mu_S + D_1\mu_R + C_2\mu_S + D_2 \geq 0 \end{array} \right\} \quad if\ D_3 \geq 0 \tag{40}$$

or

$$\left\{ \begin{array}{l} A\mu_S + B < 0 \\ C_1\mu_R\mu_S + D_1\mu_R - C_2\mu_S - D_2 \leq 0 \\ C_1\mu_R\mu_S + D_1\mu_R + C_2\mu_S + D_2 \leq 0 \end{array} \right\} \quad if\ D_3 \leq 0. \tag{41}$$

The graphical interpretation of the RS mode inequalities (40) and (41) can be shown to identical to that of the $3S$ mode. However, in the RS case, the contact wrenches of concern now are those corresponding to the two edges of the friction cone of the rolling contact and the active edge of the friction cone of the sliding contact.

4.3 Nonuniqueness of Quasistatic System Motion Prediction

Figure 3 illustrated the decomposition of the space of friction coefficients, μ-space, into regions for which the $3S$ and RS contact modes were satisfied for the example discussed in Subsection 4.1. On the boundary between the regions, both contact modes were feasible, but this ambiguity could have been resolved by a minor modification of the requirements for rolling contact. However, in this section, we present an example problem for which the

ambiguous regions of μ-space cannot be resolved by such a simple fix. This example was created by using our graphical approach to determining $3S$ and RS mode feasibility.

Figure 5 shows three contacts and the velocities of the contact points on the manipulator expressed in the contact frames. These velocities are: $\mathbf{J}_1\dot{\theta} = [0.1 \quad 0.995]^T$, $\mathbf{J}_2\dot{\theta} = [0.1 \quad -0.995]^T$, and $\mathbf{J}_3\dot{\theta} = [0.1 \quad 0.995]^T$. Again, $\mathbf{g}_{obj}$ is given as: $\mathbf{g}_{obj} = [0 \quad -1 \quad 0]^T$. The wrench matrix corresponding to the arrangement of contacts is:

$$\mathbf{W} = [\mathbf{w}_{1n} \;\; \mathbf{w}_{1t} \;\; \mathbf{w}_{2n} \;\; \mathbf{w}_{2t} \;\; \mathbf{w}_{3n} \;\; \mathbf{w}_{3t}] = \begin{bmatrix} 0.966 & -0.259 & 0.0 & -1.0 & -0.707 & -0.707 \\ 0.259 & 0.966 & 1.0 & 0.0 & 0.707 & -0.707 \\ 0.0 & -2.0 & 0.24 & -1.45 & 0.75 & -1.90 \end{bmatrix} \tag{42}$$

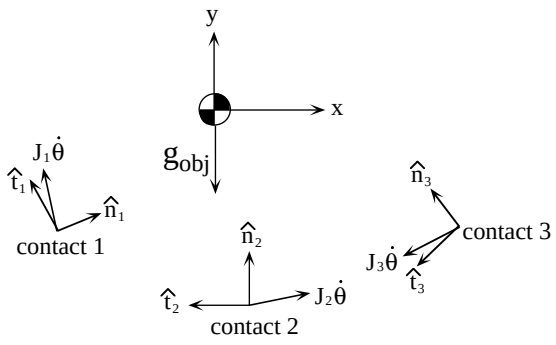

Figure 5: Configuration Admitting Multiple Consistent Contact Modes

This contact configuration and set of contact velocities admits four distinct feasible contact modes ($3S$, R_1S_3, R_2S_1, and R_3S_1), three of which are simultaneously feasible. The subscripts indicate which contact rolls and which slides. The other contact breaks.

Figure 6 shows that multiple contact modes are simultaneously feasible over large regions of friction space. Note that in Figure 6, 1's, 3's, 4's, and 6's correspond to the modes, $3S$, R_1S_3, R_2S_1, and R_3S_1, respectively. Also, for this set of contacts, the empty region near the origin is infeasible due to instability, indicating that friction is needed to maintain equilibrium.

This example leads one to believe that it is common for several contact modes to be feasible simultaneously over large regions of the parameter space associated with a given system (not just μ-space). This intuition was corroborated during the design of this example. It was clear from our graphical technique, that small but finite variations in the geometric and friction parameters and the contact points' positions and normal directions would still yield an example with multiple feasible contact modes.

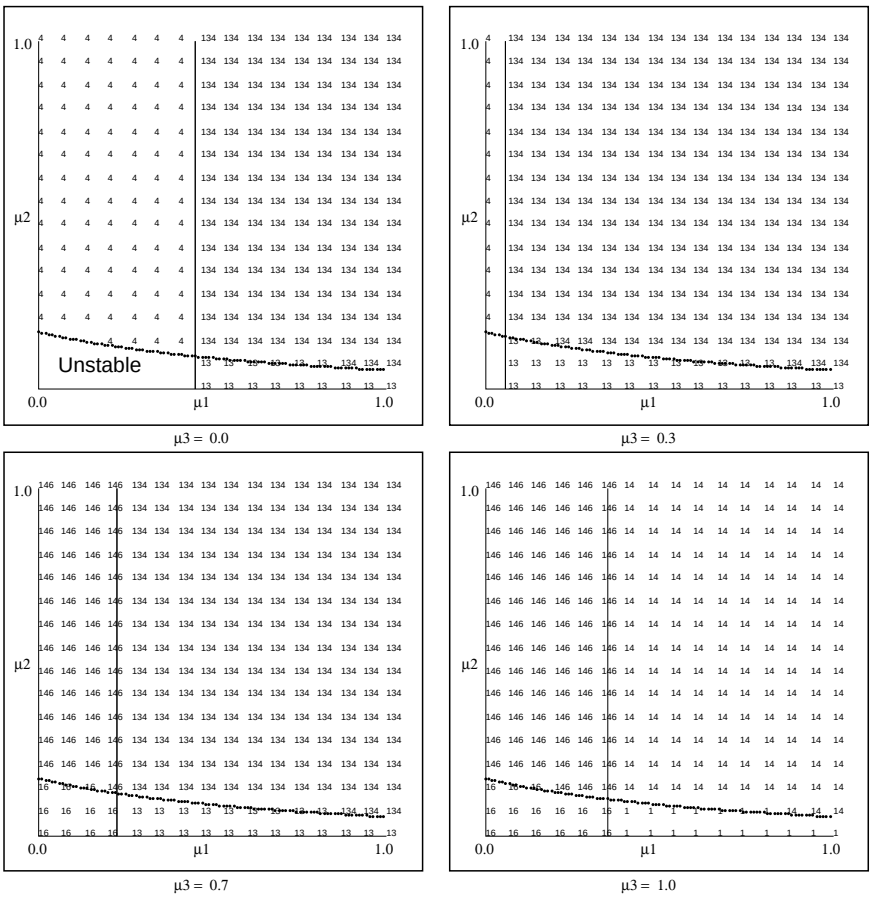

Figure 6: μ-Space Decomposition Showing Multiple Consistent Contact Modes

4.4 Regions in μ-Space for Modes $2R$, $3R$, ...

All contact modes not yet discussed have four or more applicable kinematic constraints and are therefore classified as compliant. Of those, the equilibrium equation of the modes with all rolling contacts are the simplest to map onto μ-space, because $\mathbf{W}_{A\mu}$ is independent of all friction coefficients as the following definitions show:

$$\mathbf{W}_{A\mu} = \mathbf{W}_A = [\mathbf{W}_{nR} \;\; \mathbf{W}_{tR}] \qquad \mathbf{c}_A = \begin{bmatrix} c_{nR} \\ c_{tR} \end{bmatrix} \qquad \mathbf{B}_A = \begin{bmatrix} \mathbf{U}_R & \mathbf{I} \\ \mathbf{U}_R & -\mathbf{I} \end{bmatrix}. \tag{43}$$

Assuming that $\mathbf{Q}_{A_I}^{-1}$ exists, $\mathbf{c}_A$ is independent of the coefficients of friction. Substituting into the Coulomb friction constraints gives μ-space feasibility constraints as follows:

$$c_{in}\mu_i + c_{it} \geq 0 \qquad \forall i \in \{1, 2, \cdots, n_R\} \tag{44}$$

$$c_{in}\mu_i - c_{it} \geq 0 \qquad \forall i \in \{1, 2, \cdots, n_R\} \tag{45}$$

where c_{in} and c_{it} are the following linear forms in the elements of $\boldsymbol{\tau}_I$:

$$c_{in} = \frac{\mathbf{e}_i[Adj(\mathbf{Q}_{A_I})]}{Det(\mathbf{Q}_{A_I})} \begin{bmatrix} -\mathbf{g}_{obj} \\ -\mathbf{g}_{man_I} + \boldsymbol{\tau}_I \end{bmatrix} \tag{46}$$

$$c_{it} = \frac{\mathbf{e}_{n_R+i}[Adj(\mathbf{Q}_{A_I})]_{row(n_R+i)}}{Det(\mathbf{Q}_{A_I})} \begin{bmatrix} -\mathbf{g}_{obj} \\ -\mathbf{g}_{man_I} + \boldsymbol{\tau}_I \end{bmatrix} \tag{47}$$

and the vector $\mathbf{e}_i$ selects the i^{th} row of the adjoint matrix.

Letting $n_R = n_c = 2$, inequality (44) and (45) defines the regions in μ-space for the $2R$ modes, which are applicable to two-fingered manipulation tasks. In this case, $\boldsymbol{\tau}_I$ is a scalar that can be adjusted to minimize the dependence of the workpiece's stability on friction. Abel, Holzmann, and McCarthy studied stable $2R$ grasps in the friction angle space and numerically determined curves showing the friction requirements (for stability) as a function of the internal wrench intensity [1]. The formulation given above is a generalization of their result to cases with more contacts and relates system stability directly to joint efforts. This is an advantage, because joint efforts are directly controllable in manipulator.

4.5 Regions in μ-Space for Modes $4S$, $5S$, ...

Contact modes with more than three sliding contacts and all other contacts breaking have the same definitions for $\mathbf{W}_{A\mu}$, $\mathbf{B}_A$, and $\mathbf{c}_A$ as the $3S$ modes (see equation (33)):

$$\mathbf{W}_{A\mu} = (\mathbf{W}_{nS} - \mathbf{W}_{tS}\boldsymbol{\Xi}_S\mathbf{U}_S) \qquad \mathbf{c}_A = \mathbf{c}_{nS} \qquad \mathbf{B}_A = \mathbf{I}, \tag{48}$$

but now $\mathbf{W}_{A\mu}$ is not square. The form of the μ-space constraints is similar to that of those derived during the analysis of $3S$ contact modes. The differences are that the constraints for the cases with more than three sliding contacts are of higher order (but still multilinear) in the friction coefficients and they depend (linearly) on the efforts of the effort-controlled joints.

4.6 Regions in μ-Space for All Other Modes

The mixed compliant modes do not have a simplified form. Thus their analysis requires the use of the general expressions formulated in Section 3.

4.7 Implementation

Equations (24-28) subject to the utility conditions (29-32), have been coded in 'C' using routines from IMSL's C-base library. Our implementation assumes that some planning agent has predetermined the control mode partitioning of the joints. As a result, the number of required contact constraints, $2n_R + n_S$, must be equal to the number of degrees of freedom, $3 + |\boldsymbol{\tau}_I|$, where $|\boldsymbol{\tau}_I|$ is the number of compliant (*i.e.*, effort-controlled) joints. Therefore, given the number of degrees of freedom and the number of contacts, the number of contact modes tested is:

$$\sum_{n_R=0}^{\lfloor (3+|\boldsymbol{\tau}_I|)/2 \rfloor} \begin{pmatrix} n_c \\ n_R \end{pmatrix} \begin{pmatrix} n_c - n_R \\ 3 + |\boldsymbol{\tau}_I| - 2n_R \end{pmatrix}; \quad n_c \geq (3 + |\boldsymbol{\tau}_I|)/2. \tag{49}$$

Note that there are no modes satisfying our utility conditions if n_c is less than $(3 + |\boldsymbol{\tau}_I|)/2$.

Table 1 shows the number of contact modes examined by our code as a function of n_c and it shows the approximate cpu times (on an RS6000/320) for typical problems. Notice that the numbers of contact modes tested is maximized when the number of contacts equals $3+|\boldsymbol{\tau}_I|$. However, these numbers are significantly smaller than the numbers of contact modes that would be tested (3^{n_c}) if we had not employed our utility conditions.

Number of Contacts						
n_c	3	4	5	6	7	8
Degrees of Freedom	Contact Modes Tested					
$3 + \|\boldsymbol{\tau}_I\| = n_c - 1$	6	16	45	126	357	1016
$3 + \|\boldsymbol{\tau}_I\| = n_c$	7	19	51	141	393	1107
$3 + \|\boldsymbol{\tau}_I\| = n_c + 1$	6	16	45	126	357	1016
approx. cpu seconds	0.3	0.4	0.75	2.0	5.4	15
Contact Modes Tested if no Utility Conditions are Used						
3^{n_c}	27	81	243	729	2187	6561

Table 1: Numbers of Contact Modes Tested

The largest problems that we have solved to date have had $n_c = 3 + |\boldsymbol{\tau}_I| = 12$, which required the testing of over 73,000 contact modes and used approximately 20 cpu minutes on an RS6000/320. In planning applications, the amount of time to examine one system configuration should be considerably smaller than this. Therefore, we are currently developing a new algorithm based on the bilinear programming algorithm presented in [26]. With this algorithm, we found one solution to each of several test problems with $n_c = 3 + |\boldsymbol{\tau}_I| = 20$ in several cpu seconds. Extrapolating the cpu times shown in Table 1, our enumerative algorithm would have taken approximately 3 cpu months to find all solutions for one of these problems. We emphasize, however, that the bilinear programming algorithm found *one* solution. In its current form, it terminates as soon as a solution is found. In future work, we hope to modify the algorithm so that all solutions can be found without enumerating the contact modes.

5 Finite System Motions

The above analysis has thus far been applied to specific configurations with specific velocities of the contact points on the the manipulator links. In this section, we discuss two applications in which the system motion is finite. The first application highlights changes in the contact mode during system motion, while the second application illustrates the use of quasistatic analysis to choose control inputs to select the desired contact mode when multiple modes are simultaneously feasible.

5.1 Noncompliant Contact Modes

Consider a thin rigid rod supported by two points of contact which move slowly together (see Figure 7). We assume that the coefficient of friction at contact 1 takes on a value μ_{1R} during rolling (or sticking) and a lower value, μ_{1S}, when sliding. Similarly the effective coefficient of friction at the second contact is either μ_{2R} or μ_{2S}. Of the nine possible contact modes, only two, R_1S_2 and R_2S_1, satisfy our model utility conditions. Five contact modes involve one

or more breaking contacts. These are infeasible, because equilibrium cannot be maintained. The 2R mode is kinematically infeasible since the bodies are rigid and the supports are controlled to move together continuously. The $2S$ mode fails because the rank of $\mathbf{W}_{A\mu}$ is not three.

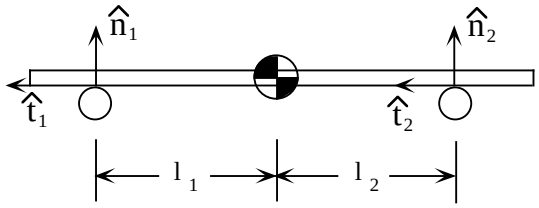

Figure 7: Thin Rod Resting on Two Moving Points

Applying inequalities (40) and (41), the R_2S_1 mode can be shown to exist if the current coefficients of friction define a point in the portion of μ-space above or on the line, $l_1\mu_2 = l_2\mu_1$ (see Figure 8). Similarly, points in μ-space below or on the line correspond to the R_1S_2 mode. Also, one can show that the $2S$ mode can occur only if the line passes through the point (μ_{1S}, μ_{2S}).

Suppose l_1 and l_2 are such that the rectangle formed by the coefficients of friction lies entirely within the R_2S_1 region as shown in Figure 8. As the supports move, l_1 will reduce, l_2 will be unchanged and the coefficients of friction will assume the values μ_{1S} and μ_{2R}, defining the upper left vertex of the rectangle. As motion progresses, the partitioning line rotates

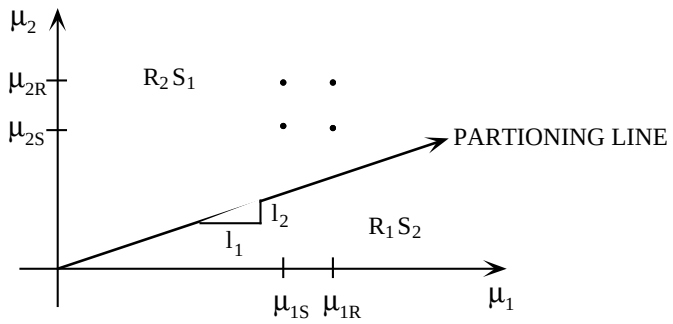

Figure 8: μ-Space Decomposition for Rod with Two Contacts

counterclockwise about the origin of μ-space. Assuming that the coefficients of friction remain fixed, then only the R_2S_1 mode is feasible until the instant the partitioning line passes through the upper left corner of the rectangle. At this point, both RS modes are feasible, but the mode must switch to R_1S_2, because if it did not, then in the next instant, the R_2S_1 mode would become infeasible with only R_1S_2 feasible. At the instant the mode switches, the coefficients of friction switch to their other values.

As the supports continue to approach each other, the partitioning line "bounces" back and forth between the upper left and lower right corners of the rectangle, switching between RS modes, seemingly chasing the current point in μ-space. The $2S$ mode is never active, because it is only feasible when the partitioning line reaches the lower left corner of the rectangle and if the coefficients of friction are equal to their sliding values, but in this example, one of the coefficients of friction is always equal to its rolling value. Note that if the coefficients of friction were random variables, with means at the corners of the rectangle, the same "bouncing" behavior would be observed, but the corners of the rectangle would not be fixed[4].

5.2 Controlling the Contact Mode with Internal Forces

Consider the planar system shown in initial and goal configurations in Figure 9. The fixed

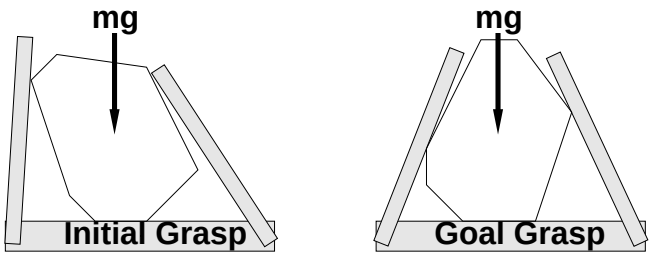

Figure 9: Initial and Goal Configurations of a Planar System

"palm" is connected to two single-link fingers whose revolute joints can be either position- or torque-controlled. In [39], we discussed an automatic planner for this system, which found coordinated joint torque and position trajectories to manipulate the workpiece from the initial grasp to the goal grasp. This plan, which was generated under the frictionless assumption, consisted of three compliant motion segments of type $4S$, each of which could be executed by position-controlling one joint while torque-controlling the other. It was shown in [39] that the controlled torque merely needed to lie within loose bounds to guarantee successful manipulation. Figure 10 shows the bounds for the first $4S$ segment of the manipulation plan, which corresponds to the fingers translating the workpiece to the left until the left finger achieves edge-to-edge contact with the workpiece (along the longest edge of the workpiece). The upper bound, which becomes infinite, is drawn as a solid bold curve which has been truncated at 200 oz.-in. The lower bound is identically zero. It is shown as a dashed bold line lying along the abscissa.

In this example, inequality (28) was used to modify the torque bounds for the $4S$ mode assuming a constant coefficient of friction, $\mu = 0.2$. The upper and lower torque bounds for this example were computed in a point-wise manner along the $4S$ trajectory segment. They are shown as bold solid and dashed curves, respectively, in Figure 11.

[4]Try this experiment with your index fingers and a ruler!

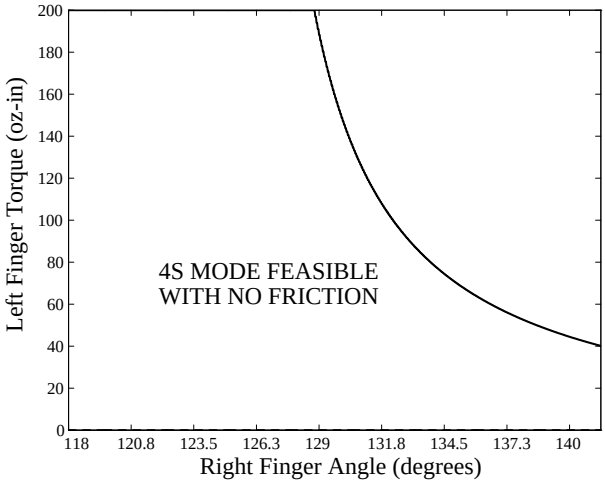

Figure 10: Torque Bounds with No Friction

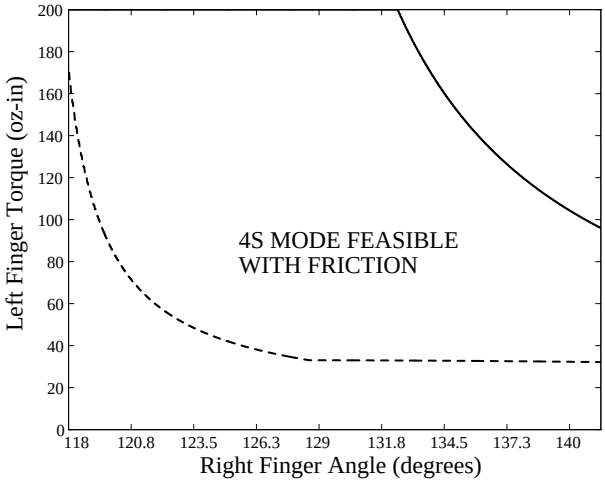

Figure 11: $4S$ Mode Torque Bounds for Friction Coefficient Equal to 0.2

Because friction is present, rolling contact modes may exist. In this example, we found one $R2S$ mode to be feasible (the one for which the object vertex on the left side of the palm rolled while the workpiece rotated counterclockwise). The bounds delineating feasibility were computed with inequality (28) formulated for that $R2S$ mode. The results are shown in Figure 12. The upper and lower bounds are again drawn as bold solid and dashed curves. Since the bounds cross about half way through the $4S$ segment, the $R2S$ mode is only feasible during the first half of the planned $4S$ segment.

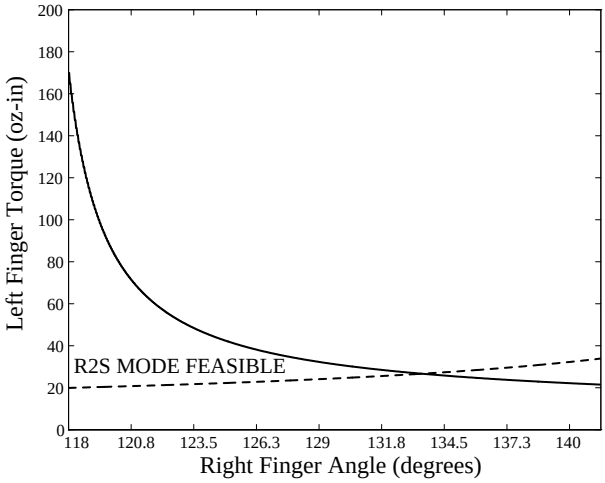

Figure 12: $R2S$ Mode Torque Bounds for Friction Coefficient Equal to 0.2

The information in the previous figures can be used to determine a set of bounds which preclude the $R2S$ mode and guarantee the $4S$ mode given that the coefficient of friction is equal to 0.2. This is the region lying above the lower bound for the $4S$ mode, above the upper bound for the $R2S$ mode, and below the upper bound for the $4S$ mode. In this particular case, the feasible regions of the contact modes do not overlap (except along a portion of the lower bound of the $4S$ region), so the region guaranteeing the $4S$ mode and precluding the $R2S$ mode is the $4S$ mode feasibility region shown in Figure 11.

Above it was assumed that the coefficient of friction was known and constant, but this is usually not the case. It is reasonable to assume that the coefficient of friction lies between known bounds. In this example, the coefficient of friction was assumed to lie in the range $[0.0, 0.2]$. The region guaranteeing the $4S$ mode despite bounded uncertainty in the coefficient of friction was found by determining the guaranteed $4S$ regions for a discrete set of friction values (we used $0, 0.01, 0.02, ..., 0.20$) and then computing the intersection of them all. The resulting region is shown in Figure 13.

These bounds were used to generate a torque control trajectory for a prototype system with teflon coated surfaces. The trajectory was successfully executed (see [32] [40] for details). It was observed that the $4S$ and $R2S$ contact modes occurred as predicted. Note that the

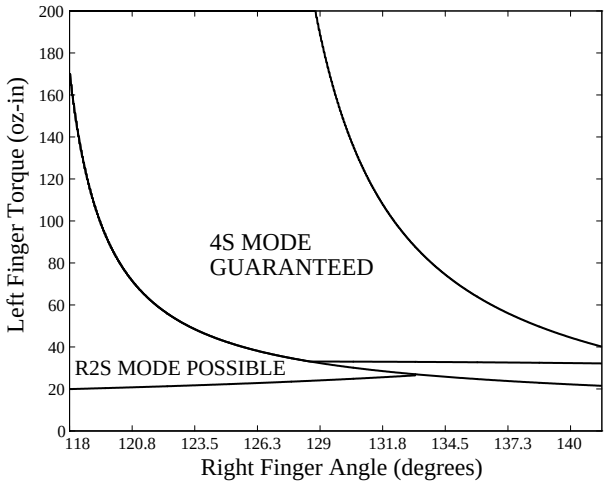

Figure 13: $4S$ Mode Guaranteed Torque Bounds for Uncertain Friction Coefficient

narrowest portion of the region specifies the resolution of the torque controller to guarantee successful execution of the $4S$ manipulation segment.

6 Conclusion

We have developed a model to predict the planar quasistatic motion of a single laminar rigid workpiece contacted at multiple points by a general planar manipulator. Our proposed solution technique tests all contact modes consistent with our proposed quasistatic model utility conditions. These conditions ensure that any quasistatic contact mode that is feasible, can remain so in the face of sufficiently small perturbations of the wrench applied externally to the workpiece. This fact is highlighted by our graphical technique which can be applied when there are either three sliding contacts or one rolling and one sliding contact.

While dynamic and quasistatic multi-rigid-body models are related, their structures have significant differences that affect their applicable solution techniques. Unfortunately, the quasistatic model shares an undesirable feature with its dynamic counterpart: more than one contact mode may be feasible for a given system state and input. This is true even when all model parameters are assumed to be known exactly. Despite such ambiguities, our results were applied successfully to two finite manipulation plans involving several moving bodies.

In the future, we plan to pursue several approaches to reducing the computation time required to find all the feasible contact modes. The first approach involves modifying our current bilinear programming algorithm to find all solutions without enumerating the contact modes. The second approach is to develop an algorithm that cleverly chooses the order

of testing the contact modes to minimize the number of column and row changes in the matrices $\mathbf{P}_{A_I}$ and $\mathbf{Q}_{A_I}$. This will allow much more efficient inversion of those matrices. The last approach is to parallelize contact mode testing, since each mode may be tested independently.

We also plan to extend our formulation to three dimensions and to include multiple workpieces. These extensions are fairly straight forward. The only complications are due to the fact that the friction cone in three dimensions cannot be represented as a system of linear inequalities. Approximating the cone by a multi-sided pyramid yields linear constraints, but presents other problems.

7 Acknowledgements

This research was supported in part by the National Science Foundation, grant nos. MSS-8909678 and IRI-9304734, the Texas Advanced Research Program, grant no. 999903-078, the Texas Advanced Technology Program, grant no. 999903-095, and NASA Johnson Space Center through the Universitys' Space Automation and Robotics Consortium, contract no. 28920-32525. Any findings, conclusions, or recommendations expressed herein are those of the authors and do not necessarily reflect the views of the granting agencies.

References

[1] J. M. Abel, W. Holzmann, and J. M. McCarthy. On grasping planar objects with two articulated fingers. In *Proceedings, IEEE International Conference on Robotics and Automation*, pages 576–581, March 1985.

[2] D. Baraff. Issues in computing contact forces for non-penetrating rigid bodies. *Algorithmica*, pages 292–352, October 1993.

[3] R. C. Brost. *Analysis and Planning of Planar Manipulation Tasks.* PhD thesis, Carnegie Mellon University School of Computer Science, January 1991.

[4] R. C. Brost and M. T. Mason. Graphical analysis of planar rigid-body dynamics with multiple frictional contacts. In H. Miura and S. Arimoto, editors, *Robotics Research: The Fifth International Symposium*, pages 293–300, Cambridge, Massachusetts, 1990. MIT Press.

[5] M. E. Caine. Chamferless assembly of rectangular parts in two and three dimensions. Master's thesis, MIT Department of Mechanical Engineering, 1982.

[6] J.J. Craig. *Introduction to Robotics: Mechanics and Control.* Addison-Wesley, second edition, 1989.

[7] M. A. Erdmann. On motion planning with uncertainty. Master's thesis, MIT Department of Electrical Engineering and Computer Science, August 1984.

[8] M. A. Erdmann and M. T. Mason. An exploration of sensorless manipulation. *IEEE Journal of Robotics and Automation*, 4(4):369–379, August 1988.

[9] R. Fearing and S. Gopalswamy. Grasping polyhedral objects with slip. In *Proceedings, IEEE International Conference on Robotics and Automation*, pages 296–301, May 1989.

[10] K. Y. Goldberg. *Stochastic Plans for Robotic Manipulation.* PhD thesis, Carnegie Mellon University School of Computer Science, November 1990.

[11] W. S. Howard and V. Kumar. A minimum principle for the dynamic analysis of systems with frictional contacts. In *Proceedings, IEEE International Conference on Robotics and Automation*, May 1993.

[12] J. Kerr. *An Analysis of Multifingered Hands.* PhD thesis, Stanford University Department of Mechanical Engineering, 1984.

[13] P. Lötstedt. Coulomb friction in two-dimensional rigid-body systems. *Zeitschrift für Angewandte Mathematik und Mechanik*, 61:605–615, 1981.

[14] P. Lötstedt. Mechanical systems of rigid bodies subject to unilateral constraints. *SIAM Journal of Applied Mathematics*, 42(2):281–296, 1982.

[15] K. Lynch. Stable pushing: Mechanics, controllability, and planning. In *Proceedings, First Workshop on Algorithmic Foundations of Robotics.* A.K. Peters, Boston, MA, 1994.

[16] K. M. Lynch. The mechanics of fine manipulation by pushing. In *Proceedings, IEEE International Conference on Robotics and Automation*, pages 2269–2276, May 1992.

[17] M. Mani and R. D. W. Wilson. A programmable orienting system for flat parts. In *North American Manufacturing Research Institute Conference XIII*, 1985.

[18] M. T. Mason. *Manipulator Grasping and Pushing Operations.* PhD thesis, Massachusetts Institute of Technology, June 1982. Reprinted in *Robot Hands and the Mechanics of Manipulation*, MIT Press, Cambridge, Massachusetts, 1985.

[19] M. T. Mason. On the scope of quasi-static pushing. In O. Faugeras and G. Giralt, editors, *Robotics Research: The Third International Symposium*, pages 229–233, Cambridge, Massachusetts, 1986. MIT Press.

[20] M. T. Mason. Two graphical methods for planar contact problems. In *Proceedings, IEEE International Conference on Intelligent Robots and Systems*, pages 443–448, November 1991.

[21] B. J. McCarragher and H. Asada. A discrete event controller using petri nets applied to assembly. In *Proceedings, IEEE International Conference on Intelligent Robots and Systems*, pages 2087–2094, 1992.

[22] V.-D. Nguyen. The synthesis of force closure grasps in the plane. Master's thesis, MIT Department of Mechanical Engineering, September 1985. AI-TR861.

[23] J. T. Oden and J. A. C. Martins. Models and computational methods for dynamic friction phenomena. *Computer Methods in Applied Mechanics and Engineering*, 52:527–634, 1985.

[24] P. Painleve. Sur les lois du frottemont de glissement. *C. R. Acad. Sci.*, 121:112–115, 1895.

[25] J.-S. Pang. personal communication, March 1994.

[26] J.-S. Pang, J. C. Trinkle, and G. Lo. A complementarity approach to a quasistatic rigid body motion problem. *Journal of Computational Optimization and Applications.* submitted February 1994.

[27] M. A. Peshkin. *Planning Robotic Manipulation Strategies for Sliding Objects.* PhD thesis, Carnegie Mellon University Department of Physics, November 1986.

[28] M. A. Peshkin and A. C. Sanderson. The motion of a pushed, sliding workpiece. *IEEE Journal of Robotics and Automation*, 4(6):569–598, December 1988.

[29] M. A. Peshkin and A. C. Sanderson. Planning robotic manipulation strategies for workpieces that slide. *IEEE Journal of Robotics and Automation*, 4(5):524–531, October 1988.

[30] V. T. Rajan. Minimum-time trajectory planning. In *Proceedings, IEEE International Conference on Robotics and Automation*, pages 758–764, March 1985.

[31] V. T. Rajan, R. Burridge, and J. T. Schwartz. Dynamics of a rigid body in frictional contact with rigid walls. In *Proceedings, IEEE International Conference on Robotics and Automation*, pages 671–677, March 1987.

[32] R. C. Ram. An implementation of a dexterous manipulator for a two-dimensional low-friction environment. Master's thesis, Texas A&M University Department of Electrical Engineering, 1993.

[33] F. Reuleaux. *The Kinematics of Machinery.* Macmillan, 1876. Republished by Dover, New York, 1963.

[34] G. Sahar and J. M. Hollerbach. Planning minimum-time trajectories for robot arms. In *Proceedings, IEEE International Conference on Robotics and Automation*, pages 751–756, March 1985.

[35] J. K. Salisbury. *Kinematic and Force Analysis of Articulated Hands.* PhD thesis, Stanford University Department of Mechanical Engineering, May 1982. Reprinted in, Robot Hands and the Mechanics of Manipulation, MIT Press, Cambridge, Massachusetts, 1985.

[36] J. M. Schimmels and M. A. Peshkin. Admittance matrix design for force-guided assembly. *IEEE Transactions on Robotics and Automation*, 8(2):213–227, April 1992.

[37] W. Seyfferth and F. Pfeiffer. Dynamics of assembly processes with a manipulator. In *Proceedings, IEEE International Conference on Intelligent Robots and Systems*, pages 1303–1310, 1992.

[38] S. Simunovic. Force information in assembly processes. In *Proceedings, 5th International Symposium of Industrial Robots*, pages 415–431, September 1975.

[39] J. C. Trinkle and J. J. Hunter. A framework for planning dexterous manipulation. In *Proceedings, IEEE International Conference on Robotics and Automation*, pages 1245–1251, April 1991.

[40] J. C. Trinkle, R. C. Ram, A. O. Farahat, and P. F. Stiller. Dexterous manipulation planning and execution of an enveloped slippery workpiece. In *Proceedings, IEEE International Conference on Robotics and Automation*, volume 2, pages 442–448, May 1993.

[41] J.C. Trinkle. On the stability and instantaneous velocity of grasped frictionless objects. *IEEE Transactions on Robotics and Automation*, 8(5):560–572, October 1992.

[42] J.C. Trinkle and R. P. Paul. The initial grasp liftability chart. *IEEE Transactions on Robotics and Automation*, 5(1):47–52, October 1989.

[43] Y.-T. Wang, V. Kumar, and J. Abel. Dynamics of rigid bodies undergoing multiple frictional contacts. In *Proceedings, IEEE International Conference on Robotics and Automation*, pages 2764–2769, May 1992.

[44] D. E. Whitney. Quasi-static assembly of compliantly supported rigid parts. *Journal of Dynamic Systems, Measurement, and Control*, 104:65–77, March 1982.

[45] D. C. Zeng. Mechanics of dexterous manipulation. Master's thesis, Texas A&M University Department of Computer Science, December 1991.

A Coefficients for the 3S Contact Mode

In this appendix, we present the definitions of the coefficients of the equations which define the regions of feasible 3S contact modes. These coefficients appear in equations (34)-(36). For the derivations of these coefficients, see [45].

$$A = -\xi_1\xi_2\xi_3 \begin{vmatrix} w_{1tx} & w_{2tx} & w_{3tx} \\ w_{1ty} & w_{2ty} & w_{3ty} \\ w_{1tz} & w_{2tz} & w_{3tz} \end{vmatrix} \qquad D = \begin{vmatrix} w_{1nx} & w_{2nx} & w_{3nx} \\ w_{1ny} & w_{2ny} & w_{3ny} \\ w_{1nz} & w_{2nz} & w_{3nz} \end{vmatrix} \tag{50}$$

$$B_1 = \xi_2\xi_3 \begin{vmatrix} w_{1nx} & w_{2tx} & w_{3tx} \\ w_{1ny} & w_{2ty} & w_{3ty} \\ w_{1nz} & w_{2tz} & w_{3tz} \end{vmatrix} \qquad B_2 = \xi_1\xi_3 \begin{vmatrix} w_{1tx} & w_{2nx} & w_{3tx} \\ w_{1ty} & w_{2ny} & w_{3ty} \\ w_{1tz} & w_{2nz} & w_{3tz} \end{vmatrix} \qquad B_3 = \xi_1\xi_2 \begin{vmatrix} w_{1tx} & w_{2tx} & w_{3nx} \\ w_{1ty} & w_{2ty} & w_{3ny} \\ w_{1tz} & w_{2tz} & w_{3nz} \end{vmatrix} \tag{51}$$

$$C_1 = -\xi_1 \begin{vmatrix} w_{1tx} & w_{2nx} & w_{3nx} \\ w_{1ty} & w_{2ny} & w_{3ny} \\ w_{1tz} & w_{2nz} & w_{3nz} \end{vmatrix} \qquad C_2 = -\xi_2 \begin{vmatrix} w_{1nx} & w_{2tx} & w_{3nx} \\ w_{1ny} & w_{2ty} & w_{3ny} \\ w_{1nz} & w_{2tz} & w_{3nz} \end{vmatrix} \qquad C_3 = -\xi_3 \begin{vmatrix} w_{1nx} & w_{2nx} & w_{3tx} \\ w_{1ny} & w_{2ny} & w_{3ty} \\ w_{1nz} & w_{2nz} & w_{3tz} \end{vmatrix} \tag{52}$$

$$E_1 = -\xi_2\xi_3 \begin{vmatrix} g_x & w_{2tx} & w_{3tx} \\ g_y & w_{2ty} & w_{3ty} \\ g_z & w_{2tz} & w_{3tz} \end{vmatrix} \qquad E_2 = -\xi_1\xi_3 \begin{vmatrix} w_{1tx} & g_x & w_{3tx} \\ w_{1ty} & g_y & w_{3ty} \\ w_{1tz} & g_z & w_{3tz} \end{vmatrix} \qquad E_3 = -\xi_1\xi_2 \begin{vmatrix} w_{1tx} & w_{2tx} & g_x \\ w_{1ty} & w_{2ty} & g_y \\ w_{1tz} & w_{2tz} & g_z \end{vmatrix} \tag{53}$$

$$F_{12} = \xi_2 \begin{vmatrix} g_x & w_{2tx} & w_{3nx} \\ g_y & w_{2ty} & w_{3ny} \\ g_z & w_{2tz} & w_{3nz} \end{vmatrix} \qquad F_{13} = \xi_3 \begin{vmatrix} g_x & w_{2nx} & w_{3tx} \\ g_y & w_{2ny} & w_{3ty} \\ g_z & w_{2nz} & w_{3tz} \end{vmatrix} \tag{54}$$

$$F_{21} = \xi_1 \begin{vmatrix} w_{1tx} & g_x & w_{3nx} \\ w_{1ty} & g_y & w_{3ny} \\ w_{1tz} & g_z & w_{3nz} \end{vmatrix} \qquad F_{23} = \xi_3 \begin{vmatrix} w_{1nx} & g_x & w_{3tx} \\ w_{1ny} & g_y & w_{3ty} \\ w_{1nz} & g_z & w_{3tz} \end{vmatrix} \tag{55}$$

$$F_{31} = \xi_1 \begin{vmatrix} w_{1tx} & w_{2nx} & g_x \\ w_{1ty} & w_{2ny} & g_y \\ w_{1tz} & w_{2nz} & g_z \end{vmatrix} \qquad F_{32} = \xi_2 \begin{vmatrix} w_{1nx} & w_{2tx} & g_x \\ w_{1ny} & w_{2ty} & g_y \\ w_{1nz} & w_{2tz} & g_z \end{vmatrix} \tag{56}$$

$$G_1 = -\begin{vmatrix} g_x & w_{2nx} & w_{3nx} \\ g_y & w_{2ny} & w_{3ny} \\ g_z & w_{2nz} & w_{3nz} \end{vmatrix} \qquad G_2 = -\begin{vmatrix} w_{1nx} & g_x & w_{3nx} \\ w_{1ny} & g_y & w_{3ny} \\ w_{1nz} & g_z & w_{3nz} \end{vmatrix} \qquad G_3 = -\begin{vmatrix} w_{1nx} & w_{2nx} & g_x \\ w_{1ny} & w_{2ny} & g_y \\ w_{1nz} & w_{2nz} & g_z \end{vmatrix}. \tag{57}$$

B Coefficients for the RS Contact Modes

In this appendix, we present the definitions of the coefficients of the equations which define the regions of feasible RS contact modes. These coefficients appear in equations (39)-(41). For the derivations of these coefficients, see [45].

$$A = -\xi_s \begin{vmatrix} w_{rnx} & w_{rtx} & w_{stx} \\ w_{rny} & w_{rty} & w_{sty} \\ w_{rnz} & w_{rtz} & w_{stz} \end{vmatrix} \qquad B = \begin{vmatrix} w_{rnx} & w_{rtx} & w_{snx} \\ w_{rny} & w_{rty} & w_{sny} \\ w_{rnz} & w_{rtz} & w_{snz} \end{vmatrix} \tag{58}$$

$$C_1 = \xi_s \begin{vmatrix} g_x & w_{rtx} & w_{stx} \\ g_y & w_{rty} & w_{sty} \\ g_z & w_{rtz} & w_{stz} \end{vmatrix} \qquad C_2 = \xi_s \begin{vmatrix} w_{rnx} & g_x & w_{stx} \\ w_{rny} & g_y & w_{sty} \\ w_{rnz} & g_z & w_{stz} \end{vmatrix} \tag{59}$$

$$D_1 = - \begin{vmatrix} g_x & w_{rtx} & w_{snx} \\ g_y & w_{rty} & w_{sny} \\ g_z & w_{rtz} & w_{snz} \end{vmatrix} \qquad D_2 = - \begin{vmatrix} w_{rnx} & g_x & w_{snx} \\ w_{rny} & g_y & w_{sny} \\ w_{rnz} & g_z & w_{snz} \end{vmatrix} \qquad D_3 = - \begin{vmatrix} w_{rnx} & w_{rtx} & g_x \\ w_{rny} & w_{rty} & g_y \\ w_{rnz} & w_{rtz} & g_z \end{vmatrix}. \tag{60}$$